UNIVERSITÀ
DEGLI STUDI
DI PADOVA

Sede Amministrativa: Università degli Studi di Padova

Dipartimento di *Scienze Cardiologiche, Toraciche e Vascolari*

Scuola di Dottorato in Scienze Mediche, Cliniche e Sperimentali
Indirizzo in Scienze Cardiovascolari
XXVIII ciclo

Mir-320a as a potential novel circulating biomarker of Arrhythmogenic Cardiomyopathy

Direttore della Scuola: Ch.mo Prof. Gaetano Thiene
Coordinatore d'indirizzo: Ch. mo Prof. Gaetano Thiene
Supervisore :Ch.ma Prof. Ssa Cristina Basso

Dottorando : Giulia Vettor

INDEX

ABSTRACT

Introduction:

The diagnosis of Arrhythmogenic Cardiomyopathy (AC) is challenging and often late after disease onset. It relies on a scoring system of major and minor criteria, requiring several clinical, instrumental and genetic tests. Diagnosis confirmation is often obtained by invasive procedures like endomyocardial biopsy and electroanatomical mapping. At present time, no circulating biomarkers are available for the diagnosis of AC.

We hypothesized that circulating microRNAs (miRNAs), which have been already demonstrated as circulating biomarkers of many cardiac diseases (e.g. heart failure, myocardial infarction, atrial fibrillation) may be used as potential diagnostic tools in AC.

Aims:

1. To screen the level of expression of miRNAs in plasma samples of AC and non-AC male subjects.
2. To assess the specificity of potential miRNAs in diagnosing AC. In particular to identify the differential expression of plasma miRNAs in AC patients vs. healthy controls (HC) and/or patients with ventricular arrhythmias of different aetiologies: idiopathic ventricular arrhythmias (IVT) and patients with ischemic ventricular arrhythmias (IC).
3. To evaluate a possible correlation between miRNAs expression and the severity of the disease in terms of ventricular function and fibro-adipose replacement of the myocardium by means of ElectoAnatomic voltage Mapping [EAM] and Late Gadolinium Enhancement (LGE) detected by Contrast Enhancement Cardiac Magnetic Resonance (CE-CMR)
4. To assess in cardiac stromal mesenchimal cells culture how different levels of expression of the identified miRNAs may regulate the onset and progression fibro-adipogenesis.

Methods:

All patients with a history of ventricular arrhythmias referred to Arrhythmia Center of the Cardiology Center Monzino (Milan), for transcatheter ablation were enrolled in the study as well as a control cohort of patients matched in terms of age and sex.

All patients underwent:

- CE-CMR evaluating the volumes and function of the right and left ventricle (RV and LV), the presence and extension of LGE;
- Electroanatomic voltage mapping (CARTO) of RV and LV.
- Endomyocardial biopsy, when indicated, to evaluate the presence and extension of fibro-fatty infiltration of the RV.
- Blood sampling for molecular analysis of 320 miRNA expression.

Blood samples (5ml) were collected in EDTA coated tubes and the total RNA was extracted from plasma. The expression of each single miRNA was evaluated using TaqMan microRNA assays (Life Technologies) following manufacturer's instructions. Validated miRNAs expression data were analyzed using GraphPad Prism version 5.03 for Windows and reported as mean ± standard deviation of the mean (SD). Cardiac Mesenchymal Stromal Cells (C-MSCs) from AC ventricular samples have been obtained in our laboratory and have been used as *in vitro* model of AC and we decided to evaluate miR-320a in this model. In order to assess C-MSCs involvement during adipogenesis we planned an *in vitro* experiment to simulate AC development. We maintained the same plated number of C-MSCs in adipogenic medium for 3 days.

Results:

In the present study a total of 114 male subjects were enrolled: 35 patients were affected by AC, 35 were HC, 20 were affected by IVT and 24 were affected by IC.

The level of expression of 368 miRNAs was screened in plasma of 3 symptomatic AC patients and 3 age- and sex-matched healthy donors: 150 miRNAs were found expressed in all screened plasma samples and 14 miRNAs resulted putatively regulated.

Among the top 4 regulated miRNAs, considering both relative fold change and statistical significance, miR-320a was confirmed to be regulated in an initial validation step, performed by qRT-PCR in the plasma of 16 HC and 16 AC patients, as defined by current

guidelines. Therefore its expression was analyzed in all HC and AC patients. MiR-320a showed a statistically significant lower expression in AC patients compared to HC (0.42±0.04, p=0.008) and with a cut-off value of ΔCt <-5.55 presented a sensitivity of 65% specificity of 80% to discriminate AC patients.

We did not find any statistical significance in the level of expression of miR-320a between HC and IVT (fold 1.09±0.5 p=ns) as well as between HC and IC (fold 0.74±0.22 p=ns).

In evaluating the expression of miR-320a in terms of the severity of the disease in patients with AC we did not find any statistically significant correlation with major arrhythmic events as well as no correlation with RV function. A significant correlation was found between impairment of the LV function and ΔCt expression (r^2=0.20 p<0.04).

Evaluating miR-320a expression in 12 patients with AC we found a trend of statistically significance with the extension of scar areas detected by unipolar electroanatomic mapping and LGE (p=0.07).

The results from the *in vitro* study on C-MSC, showed a lower expression of miR-320a in AC C-MSCs compared to non-AC C-MSCs (0.44±0.08, p=ns).

Conclusions:

This is the first study that evaluates the diagnostic potential of circulating miRNAs in AC. Plasma levels of mir-320a are consistently lower in AC patients compared to HC, IVT and IC subjects and has a fairly good accuracy in discriminating AC vs. IVT patients. Low miR-320a plasma concentrations may represent a new potential biomarker for AC. Plasma concentration of miR-320a seems to demonstrate an inverse correlation with AC severity. MiR-320a regulation in a cardiac cellular model of AC during induced adipogenesis may pave the way to future mechanistic studies on the epigenetic control of AC adipogenesis.

Introduzione:

La diagnosi di Cardiomiopatia Aritmogena (CA) risulta essere spesso una sfida per il cardiologo clinico e viene talvolta effettuata in ritardo rispetto all'insorgenza dei sintomi. Si basa sull'identificazione di criteri diagnostici ottenuti attraverso l'utilizzo di diverse indagini clinico-strumentali, talvolta invasive e tramite test genetici. Ad oggi nessun marcatore bioumorale circolante è stato validato e utilizzato quale criterio diagnostico.

Abbiamo ipotizzato che i microRNA (miRNA) circolanti, già validati nella diagnosi di molte altre malattie cardiache (insufficienza cardiaca, infarto miocardico, fibrillazione atriale) possano essere utilizzati come potenziale strumento diagnostico nella CAVD.

Obiettivi:

1. Eseguire uno screening di miRNA in campioni di plasma di soggetti maschi sani o affetti da CA.
2. Valutare la specificità e la sensibilità dei miRNA nel riconoscimento della CA. In particolare identificare i diversi livelli d'espressione dei miRNA plasmatici nei pazienti con CA rispetto ai controlli sani (CS) e/o ai pazienti con aritmie ventricolari a diversa eziologia (tachicardia ventricolare idiopatica (TVI) o conseguente a cardiopatia ischemica (CI).
3. Valutare la possibile correlazione tra l'espressione dei miRNA e la gravità della malattia espressa in termini di numerosità degli eventi aritmici maggiori, funzionalità ventricolare destra e sinistra e in termini di estensione della sostituzione fibro-adiposa ottenuta mediante mappaggio elettroanatomico e risonanza magnetica cardiaca (RMC).
4. Valutare come la differente espressione dei miRNA circolanti identificati possa regolare lo sviluppo e la progressione della sostituzione fibro-adiposa in colture di cellulle cardiache mesenchimali stromali (C-MSC).

Metodi:

Sono stati arruolati nello studio tutti i pazienti con aritmie ventricolari, riferiti all'Unità di Elettrofisiologia del Centro Cardiologico Monzino (Milano) per essere sottoposti ad ablazione transcatetere e controlli sani.

Tutti i pazienti sono stati sottoposti a:

- RMC per valutazione dei volumi e funzionalità del ventricolo destro e sinistro e per determinazione dell'estensione delle "scars".
- Mappaggio elettroanatomico intracavitario bipolare e unipolare (CARTO).
- Biopsia endomiocardica, quando indicata per valutazione della presenza e l'estensione della sostituzione fibro-adiposa del ventricolo destro.
- Prelievo di sangue venoso l'analisi molecolare di 320 miRNA.

I campioni di sangue (5 ml) sono stati raccolti in provette EDTA e l'RNA totale è stato estratto dal plasma. L'espressione di ogni singolo miRNA è stata valutata utilizzando saggi TaqMan microRNA (Life Technologies) seguendo le istruzioni del produttore. L'espressione dei MiRNA validati è stata analizzata utilizzando GraphPad Prism versione 5.03 per Windows e riportati come media ± deviazione standard della media (SD). Le cellule stromali mesenchimali cardiache (C-MSC) sono state ottenute da un campione bioptico di pazienti con sospetta CA. Al fine di valutare il coinvolgimento C-MSC durante adipogenesi è stato eseguito un esperimento in vitro per simulare lo sviluppo della patologia.

Risultati:

114 soggetti maschi sono stati arruolati nello studio: 35 soggetti affetti da CA, 35 soggetti sani, 20 affetti da TVI e 24 da CI.

Il livello d'espressione di 368 miRNA circolanti è stato valutato su campioni di plasma di 6 soggetti (3 affetti da CA e soggetti sani).

Di 150 miRNA espressi in tutti i campioni di plasma, 14 miRNA sono risultati regolati.

Tra i 4 miRNA maggiormente regolati, il miR-320a è stato validato inizialmente mediante qRT-PCR nel plasma di 32 soggetti (16 controlli sani e 16 soggetti affetti da CA)

In seguito abbiamo valutato l'espressione di miR-320a in tutti i soggetti dello studio.

I livelli d'espressione del miR-320A sono risultati statisticamente inferiori nei soggetti affetti da CA rispetto ai controlli sani (0,42 ± 0,04, p = 0,008) con un valore di cut-off (ΔCt <-5.55) il miR-320a ha presentato una sensibilità del 65% e una specificità dell' 80% nel discriminare I pazienti con CA.

Non abbiamo trovato nessuna differenza statisticamente significativa nell'espressione di miR-320a tra soggetti sani e affetti da TVI (1,09 ± 0,5 p = ns) come tra soggetti sani e affetti da CI (0.74 ± 0.22 p = ns).

Nei soggetti affetti da CA, non abbiamo trovato alcuna correlazione tra i livelli d'espressione di miR-320 a e il verificarsi di eventi aritmici maggiori così come con gli indici di funzionalità ventricolare. Una correlazione statisticamente significativa è stata riscontrata tra i livelli di espressione del miR-320a e la funzione ventricolare sinistra (FE)(r^2=0.20 p<0.04).

In 12 dei pazienti con CA abbiamo trovato un trend di significatività statistica tra i livelli di miR-320 a e le aree di "scar" al mappaggio elettroanatomico unipolari e la presenza di LGE (p=0,07).

Dallo studio in vitro sulle C-MSC abbiamo evidenziato una ridotta espressione di miR-320 nelle cellule ottenute dai pazienti con CA rispetto alle cellule ottenute dagli altri soggetti (0,44 ± 0,08, p=ns)

Conclusioni:

Questo è il primo studio in cui sia stata valutata l'utilità diagnostica dei miRNA circolanti nella CA. I livelli plasmatici d'espressione del miR-320a sono costantemente più bassi nei soggetti affetti da CA rispetto a soggetti sani o con cardiopatia ischemica o affetti da tachicardia ventricolare idiopatica e si è dimostrato in grado di discriminare con una buona accuratezza i soggetti affetti da CA rispetto ai soggetti affetti da TVI.

I nostri dati preliminari suggeriscono miR-320a quale potenziale marcatore bioumorale di CA e sembrerebbero evidenziare una correlazione inversa tra i livelli d'espressione di miR-320a e la gravità della patologia.

La creazione di un modello cellulare di adipogenesi indotta in cellule mesenchimali stromali cardiache mediante regolazione di miR-320a potrebbe aprire la strada a futuri studi meccanicistici sul controllo epigenetico dell'adipogenesi nella CA.

INTRODUCTION

1. Arrhythmogenic Cardiomyopathy

1.1 Definition

Arrhythmogenic Cardiomyopathy (AC) is a rare, genetic, inherited heart muscle disease, that is a main cause of sudden cardiac death (SCD) due to ventricular arrhythmias, especially in younger than 35 years and athletes[1].

It was first described in 1736 by the Pope's physician, Giovanni Maria Lancisi, in his book entitled "*De Motu Cordis et Aneurysmatibus*". He reported that there was a family who had experienced pathologic right ventricle (RV), heart failure (HF) and SCD in four generations.

The first comprehensive clinical description of the disease was reported by Marcus *et al.* in 1982, when he reported 24 adult cases with ventricular tachyarrhythmias with left bundle branch morphology[2].

AC has undergone several name changes. It was initially identified by Fontaine *et al.* as a pre-excitation syndrome, later was considered a dysplastic disorder and further expanded to include the arrhythmic features to become Arrhythmogenic Right Ventricular Dysplasia (ARVD)[3]. It is recently considered a cardiomyopathy and called "Arrhythmogenic Right Ventricular Cardiomyopathy" (ARVC)[4]. Nowadays the encompassing term "Arrhythmogenic Cardiomyopathy" (AC) is increasingly used in order to considerate the whole spectrum of the disease than the only "right forms", because there are many evidence of biventricular or even isolated left ventricular forms[5].

1.2 Pathology

The main aspect of the disease is the progressive replacement of the right ventricular myocardium by fibrous and fibro-adipose tissue, starting from the epicardium and extending to the endocardium as to become transmural (Figure 1). In addition, the myocardium usually shows a marked atrophy at the free wall, accounting for thinned and translucent appearance of the wall, even though the distance between the epicardium and the endocardium may be preserved[1].

The fibro-adipose replacement interferes with electrical impulse conduction and is the key cause of electrocardiographic typical features as epsilon waves, left or right bundle branch block (LBBB, RBBB), late potentials, life-threatening re-entrant ventricular arrhythmias and progression towards HF.

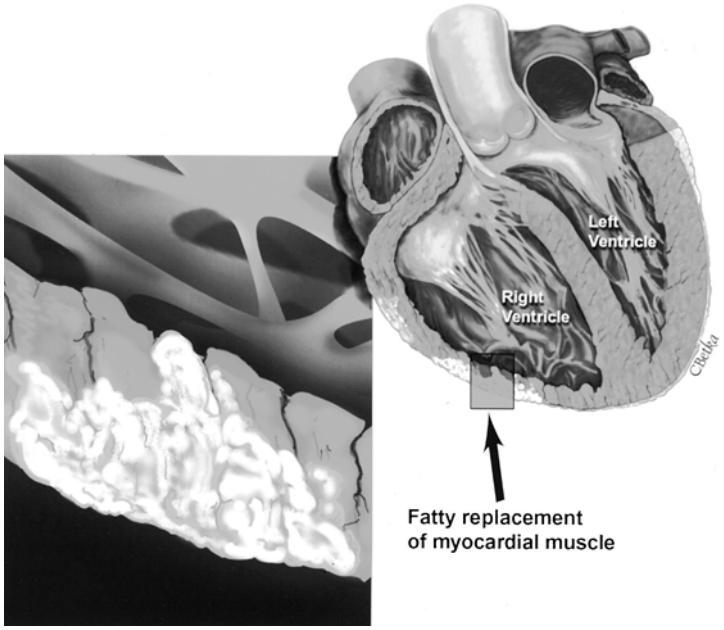

Figure 1 | Illustration of adipose replacement of myocardium within the right ventricular wall[6].

Schematic illustration of adipose infiltration and substitution starting from the epicardium and extending to the endocardium as to become transmural.

AC may have a broader phenotypic spectrum with biventricular forms and in 5% of cases with predominant involvement of the left ventricle. The latter case, most frequently in aged patients, is associated with marked cardiomegaly and increased risk of

arrhythmias and heart failure (HF). In the early prodromal stage of the disease, called "concealed phase" structural changes may be absent or subtle and confined to a localized region of the RV, typically the inflow tract, outflow tract, or apex of the RV, at the so called "triangle of dysplasia"[7]. Progression to more diffuse RV disease and left ventricular (LV) involvement, typically affecting the posterior lateral wall, is common, but disease expression is variable. Trans mural atrophy of the myocardium causes aneurysmal dilatation and wall motion abnormalities and lead, in advanced stages, to HF. In the "concealed phase", individuals are often asymptomatic, but SCD may, occasionally, be the first symptom[8, 9].

The histologic pattern, typical of the disease, is a progressive degeneration of myocytes and consequent accumulation of fibro- and fibro-adipose tissue (Figure 2). These changes are often associated with the presence of inflammatory infiltrates (Figure 2). It is not yet clear whether the inflammation is caused by a reaction to apoptotic death of myocytes or whether it results from viral infections or immune reactions.

The ultimate phenotype may resemble dilated cardiomyopathy.

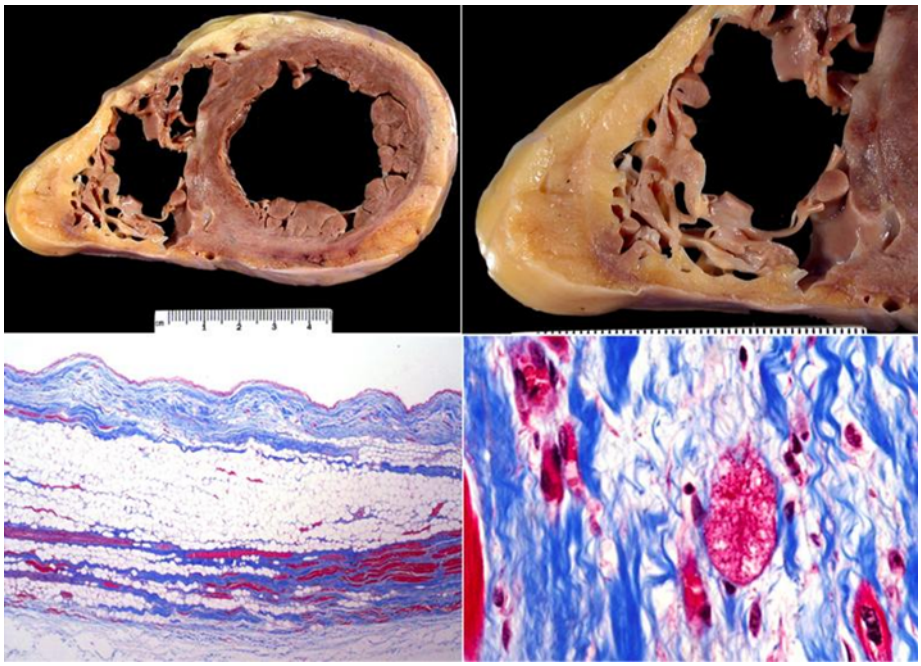

Figure 2 | Autopsy heart in a young man who died suddenly playing basketball [10].

Top left demonstrates increased fat in the outer walls of the right ventricle and left ventricular posterolateral walls. A higher magnification of the right ventricle is seen at the top right image; the anterior wall is nearly

completely replaced with fat, and fibro-adipose irregular posterior wall involvement is seen. The bottom left image demonstrates a full thickness of the right ventricle stained with Masson trichrome. The residual muscle is present only in a band-like area of scarring, and subepicardial scarring is present as well. The characteristic myocyte vacuolization, depicted in the bottom right image, is seen in nearly all areas of ARVC within the scarred areas.

Most of the information on AC comes from studies of the usual form of the disease with predominant RV involvement. However, recognition of a disease pattern characterized by early and predominant LV involvement has increased. The left-dominant AC (LDAC) pattern should not be confused with the well-known LV involvement observed in the advanced stages of AC, as a result of disease progression. Clinical markers of LDAC include ECG abnormalities that suggest left-side involvement, such as lateral or inferolateral T-wave inversion (leads V5, V6, LI, and aVL)[11], and ventricular arrhythmias of right bundle branch block morphology that suggests an LV origin. True LDAC mirrors classic right-dominant AC, with the left ventricle more-severely affected than the right ventricle (an RV/LV volume ratio <1).

A far more-sensitive indicator of left-sided disease is late gadolinium enhancement, which is frequently detected in a segment without a concomitant wall-motion abnormality, and thus precedes the onset of LV dysfunction or dilatation. Typically, LV late gadolinium enhancement involves the inferolateral and inferoseptal regions, and affects the subepicardial or midwall layers, similar to the histological pattern of fibrofatty myocardial replacement observed at post-mortem examination[12]. Septal late gadolinium enhancement is present in >50% of cases of LDAC, unlike the right-dominant classical pattern in which septal involvement is unusual. Differential diagnosis of dilated cardiomyopathy in patients with suspected AC is mandatory for risk-stratification and familial-evaluation purposes. The main distinction in LDAC is a propensity to electrical instability that exceeds the degree of ventricular dysfunction, compared with dilated cardiomyopathy, where ventricular arrhythmias and sudden cardiac death occur in the context of overt systolic dysfunction with symptoms of heart failure. Moreover, regional involvement (by contrast with the global involvement in dilated cardiomyopathy) is suggestive of AC, particularly when RV abnormalities are prominent.24 Importantly, patients with a moderate-to-severe decrease in LV function were excluded from a diagnosis of AC by the 1994 Task Force criteria, but this restriction has been eliminated in

the 2010 criteria. As recognized by the Task Force, awareness is growing that classic AC with RV involvement is the most well-recognized variant of a broad spectrum of disease that includes LDAC and biventricular subtypes. The lack of specific diagnostic guidelines contributes to the under-recognition of these nonclassical variants of AC. Future revisions of the Task Force criteria will need to address this disparity, by incorporating features such as ventricular tachycardia of right bundle branch block morphology, subepicardial or midmyocardial late gadolinium enhancement of the LV myocardium, and global or regional LV dysfunction in patients who present with arrhythmia rather than heart failure[13].

1.3 Incidence

AC is a rare primitive myocardial disease with an estimated prevalence of 1:5,000 in the worldwide population[14, 15]. Interestingly, it is more diffuse in the north of Italy; in Veneto it reaches the peak of 1:2,000[16, 17]. Men are more frequently affected then women in a ratio of 3:1[18]. AC is a devastating disease given that the first symptom is often SCD. Data from literature indicate that 11-22% of cases of SCD in young athletes (<35 years) occurred during physical exercise are due to the undiagnosed presence of AC[16].

1.4 Genetics

More than a decade elapsed between the recognition of familial AC, and the identification of the first disease-causing gene mutation. The difficulty in identifying affected individuals in the families of patients with AC, mostly because of the variable penetrance and the low sensitivity of diagnostic criteria in the familial forms of the disease, represented a major obstacle to early linkage-mapping studies and subsequent candidate-gene evaluation.

For the first time, in 1994, a disease locus was identified in chromosome 14 by linkage analysis in large families with dominant AC. Later in the year 2000 was an AC-causing gene mutation identified in *JUP* in a fully penetrant, autosomal-recessive form of the disease with an easily recognizable cardiocutaneous phenotype (Naxos disease). A recessive mutation in *DSP* was subsequently found to cause another cardiocutaneous syndrome, Carvajal disease, which is characterized at the cardiac level by biventricular

involvement. Therefore, after many years of linkage-analysis studies that led to the identification of several disease loci, but no disease genes, the molecular basis of AC was discovered by investigation of cardiocutaneous syndromes. In particular, a morphological study of the heart of a patient with Carvajal disease, showed biventricular wall thinning with aneurysms, myocardial atrophy, and fibrosis, which immediately suggested that the disease-causing gene mutations involved in that cardiocutaneous syndrome might also be ideal candidates for the autosomal-dominant form of AC. Consequently, in 2002, mutations in the *DSP* gene were identified in families that had been followed up since the 1980s in an outpatient clinic in Padua, Italy.

Subsequently, a variety of mutations have been found in other desmosomal genes, including *PKP2*, *DSG2*, and *DSC2*. Mutations in *JUP* have been reported even in dominant forms of AC, and in *DSC2* and *PKP2* in recessive variants of the disease. With the exception of a few genes unrelated to the cell-adhesion complex, such as *RYR2* (encoding the ryanodine receptor 2), *TGFB3* (transforming growth factor β_3), and *TMEM43* (transmembrane protein 43, also known as protein LUMA), the most-common disease-causing mutations occur in genes that encode desmosomal proteins. Mutations in *DES* (desmin) and *TTN* (titin) have been proposed as novel causes of AC.

In about 30-50% of cases AC has a familiar occurrence, usually with an autosomal dominant inheritance pattern, with low penetrance and variable expressivity[19].

A rare autosomal recessive variant of the disease, called Naxos disease shows similar myocardial involvement with typical palmoplantar keratosis and wooly hair[20].

1.4.1 Desmosomal mutations

Approximately 50% individuals, affected by the familial form of the disease, harbour an autosomal dominant mutation in one of the five genes coding for components of the cardiac desmosome: desmoplakin (*DSP*)[21], plakoglobin (*JUP*)[22], plakophilin 2 (*PKP2*)[23, 24], desmoglein 2 (*DSG2*)[25], and desmocollin 2 (*DSC2*)[26] (Figure 3, Table 1). Recessive mutation of *DSP* and *JUP* has been reported associated with cardiocutaneous disease, the Carvajal syndrome [21] and the Naxos disease, respectively[27].

Desmosomes are complex cellular junctions located between adjacent cells with structural and intracellular signalling function. Cell adhesion junctions preserve the

proper function and structure of cardiac myocytes and epithelial cells of the skin in the intercalated disks. The intercalated disk contains three different intercellular connections: gap junctions, responsible for electric coupling between cells, adherens junctions, and desmosomes both of which provide mechanical coupling by linking the cytoplasmic actin and intermediate filaments, respectively. Furthermore, desmosomes play a crucial role in organising and maintaining intercalated disks, thereby determining the preservation of the electrical coupling between cells.

Diseases related to mutations in these proteins are manifested mainly in cardiac and epitelial tissues, due to the continuous mechanical stress of the myocardium and the epitelium that alters the cellular biomechanical behaviour.

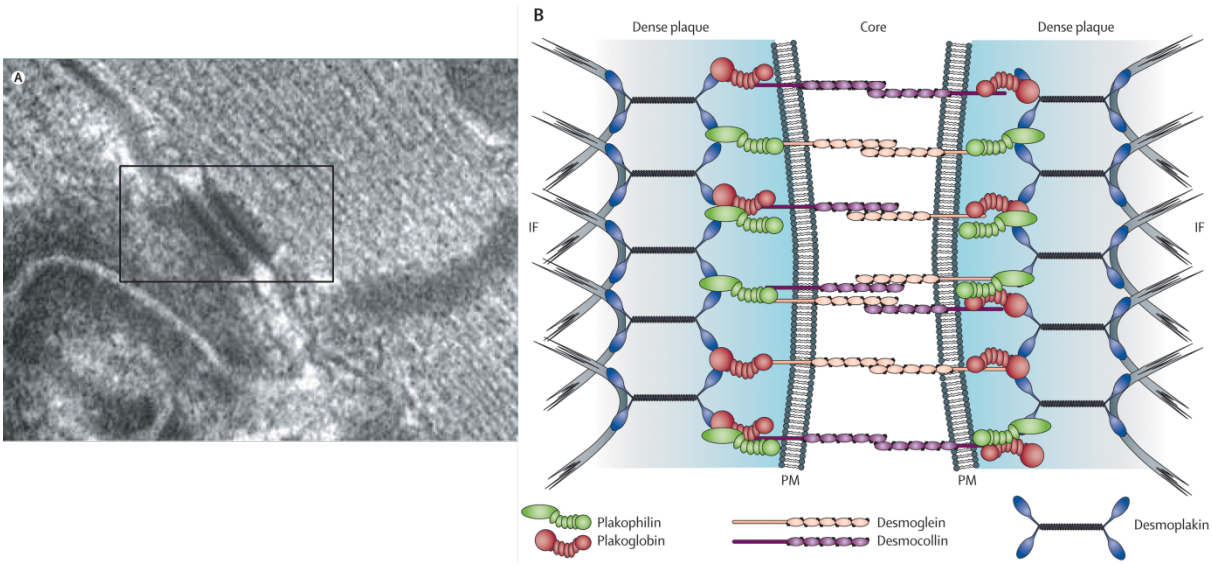

Figure 3 | Intercellular mechanical junction (desmosome) of the cardiomyocyte [28].

(A) Transmission electron microscopy of cardiomyocyte desmosome. (B) Schematic representation of desmosome components. Core region mediates cell-cell adhesion and dense plaque provides attachment to the intermediate fi laments. There are three major groups of desmosomal proteins: transmembrane proteins (desmosomalcadherins) including desmocollins and desmogleins; desmoplakin, a plakin family protein that binds directly to intermediate fi laments (desmin in the heart); and linker proteins (armadillo family proteins) including plakoglobin and plakophilins which mediate interactions between the desmosomal cadherin tails and desmoplakin. IF=intermediate fi laments. PM=plasma membrane.

Indeed, the prevailing hypothesis on desmosomal gene mutations causing AC is based on the effect of mechanical stress leading to the weakness of the intercellular junction causing disruption and degeneration of myocytes followed by inflammation and

reparative phenomena, which would lead to myocytes replacement, by fibro- and fibro-adipose scar tissue (Figure 4). In this structural model, environmental factors such as exercise or inflammation could exacerbate impairment of cell adhesion and hasten disease progression.

The right ventricle (RV) is considered more susceptible to damage than the left one both due to its lower thickness of the walls and the physiological response dilated paid to the exercise. Environmental factors such as exercise or inflammation caused by viral infections may further weak desmosome structures accelerating AC progression.

Moreover, the fibro-adipose substitution could be mediated by signalling interfering with the Wnt/β-catenin pathway [29].

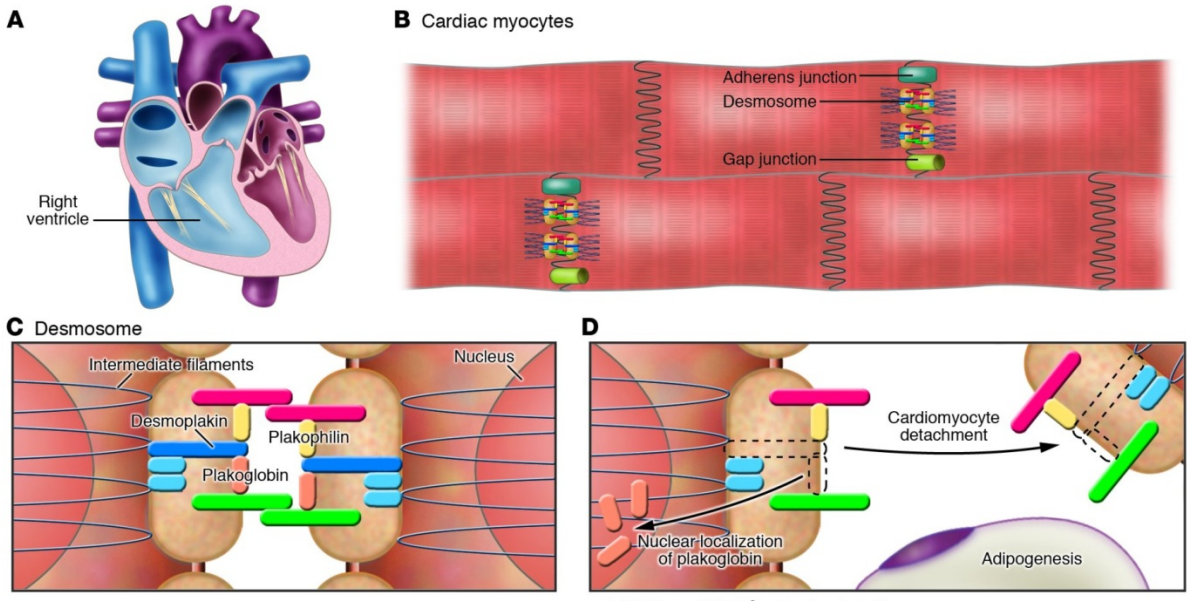

Figure 4 | Cardiac-specific restriction of the desmosomal protein desmoplakin causes nuclear localization of plakoglobin and reduced Wnt/β-catenin signaling, recapitulating human ARVC [30].

AC predominantly affects the right ventricle of the heart. (B) The intercalated discs of cardiac myocytes are characterized by gap junctions, adherens junctions, and desmosomes. (C) Cell-cell adhesion is largely dependent on interaction of intracellular components of the desmosomal plaque such as desmoplakin and plakoglobin. (D) Plakoglobin delocalization and Wnt/β-catenin signaling reduction in mice cause increased expression of adipogenic and fibrogenic genes in vitro, abnormal cardiac adipose tissue and fibrosis in vivo, and ventricular arrhythmias similar to human AC. Interactions between signaling defects and mechanical stresses are likely to be involved in the genesis of the final phenotype.

1.4.2 Non-desmosomal mutations

Mutations in genes encoding non-desmosomal proteins are also implicate in AC. Mutations in the 5' or 3' untranslated region of the transforming growth factor beta 3 gene (*TGFB3*) have been described in AC patients. These mutations led to increased expression of TGFB3, which has a pro-fibrotic effect (Table 1) [31].

Missense mutations in the gene encoding the cardiac ryanodine receptor (*RYR2*) (Table 1), a calcium release channel in the sarcoplasmic reticulum, have been described in Italian families with a distinct form of AC characterised by exercise-induced ventricular arrhythmias and a high penetrance [32]. RYR2 mutations have also been identified in families with catecholaminergic polymorphic ventricular tachycardia (CPVT) [33], rising suspicion of phenocopy.

Another founder mutation has been recognized in the gene encoding the transmembrane protein 43 (TMEM43) (Table 1) [34], which cause a form of AC found to be fully penetrant with prominent LV involvement. Notably, men carrying this mutation are prone to exacerbate the disease at a younger age than women. It has been hypothesized that the TMEM43 mutation causes fibro-adipose replacement of the myocardium inducing the activation of the adipogenic transcription factor PPARγ.

In 2010, Klauke et al. identified a case of missense mutation in the gene encoding for desmin (*DES*) (Table 1) [35]. Desmin is a cytoskeletal filament protein located in the myocardium at the intercalated disk, and connected to the desmosomal plaque proteins via desmoplakin, thus supporting the resistance to mechanical stress of cardiomyocytes [36]. Mutations in *DES* gene are often involved in skeletal abnormalities.

Recently, Taylor and colleague identified in the gene coding for titin (*TTN*) (Table 1) a missense variant segregating in an AC family [37]. Titin, after myosin and actin, is the third most abundant protein of striated muscle, and connects the Z-line to the M-line in the sarcomere [37-39].

To date 15 mutations in the Phospholamban (*PLN*) (Table 1) gene, a regulator of the SERCA pump, has been described in association both with dilated cardiomyopathy (DCM) and AC [40].

Finally in 2012, four Lamin A/C (*LMNA*) (Table 1) pathogenic variants were linked to clinically severe forms of AC and to one case of sudden death. Therefore, this gene was added to the database as associated with AC [41].

Chromosome locus	Gene	Protein	Inheritance	Disease
Desmosomal genes				
17q21	***JUP***	Junction plakoglobin	AR	Naxos associated disease
17q21	***JUP***	Junction plakoglobin	AD	
6p24	***DSP***	Desmoplakin	AR	Carvajal syndrome
6p24	***DSP***	Desmoplakin	AD	LV involvement
12p11	***PKP2***	Plakophilin 2	AD, AR	
18q12	***DSG2***	Desmoglein 2	AD	LV involvement
18q12	***DSC2***	Desmocollin 2	AD, AR	
Extra-desmosomal genes				
1q42–q43	***RYR2***	Ryanodine receptor 2	AD	CPVT phenotype
14q23–q24	***TGFB3***	Transforming growth factor β 3	AD	
3p25	***TMEM43***	Transmembrane protein 43	AD	
2q35	***DES***	Desmin	AD	DCM and HC phenotype, early conduction disease
2q31	***TTN***	Titin	AD	Early conduction disease, AF
1q11-q23	***LMNA***	Lamin A/C	AD	DCM phenotype
6q22.1	***PLN***	Phospholamban	AD	DCM phenotype

Table 1 | Schematic list of mutations involved in AC.

AD=Autosomal Dominant; AR=Autosomal Recessive; LV=Left Ventricle AF=Atrial Fibrillation; CPVT=Catecholaminergic Polymorphic Ventricular Tachycardia; DCM=Dilated Cardiomyopathy HC=Hypertrophic Cardiomyopathy.

1.5 Wnt pathway

Wnt signalling controls various cellular and biological processes, such as cellular adhesion [42, 43], self-renewal [44], cancer development [45, 46], differentiation [47], cell polarity, migration, proliferation and development of various tissues [48, 49].

Wnts are secreted glycoproteins that signal through Frizzled (Fz) receptors [50] and low density lipoprotein receptor-related protein (LRP) co-receptors [51] in order to play autocrine and paracrine effects on cellular differentiation and growth.

When Wnt signalling is active glycogen synthase kinase 3 (GSK3) is inhibited. This loss of GSK3 activity allows cytosolic β-catenin to accumulate and translocate to the nucleus where it binds to the T-cell factor (TCF)/lymphoid-enhancing factor family of transcription factors and activates transcription of Wnt-regulated target genes [52]. On the other hand, when Wnt signalling is suppressed GSK3 phosphorylates β-catenin and targets it for ubiquitin-mediated degradation [53]. Moreover, this pathway controls adipogenic differentiation of pre-adipocytes [54], it is a key regulator during cardiac development and injury [55], and it represents regulatory mediators of the perturbed metabolic activities of cancer cells.

Interestingly, plakoglobin (γ-catenin) has approximately 85% sequence identity to β-catenin. It has been suggested that their competition for DNA binding leads to suppression of Wnt signalling and to transcriptional switch to adipogenesis [29, 56]. Furthermore, both nuclear localisation of plakoglobin and reduced canonical Wnt/β-catenin signalling have been proposed to contribute to AC adipogenesis [29].

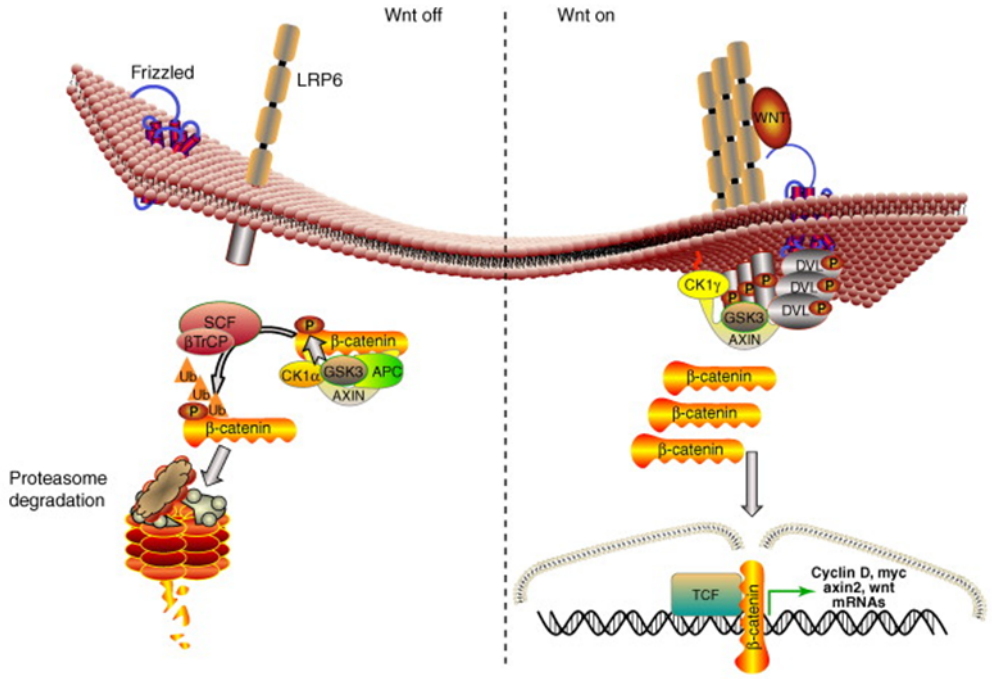

Figure 5 | General overview of Wnt/β-catenin signaling (MacDonald, Tamai, et al.).

In the absence of Wnt (Wnt off), CK1α/GSK3 phosphorylation of β-catenin ensures that cytoplasmic β-catenin is continually targeted for ubiquitin-mediated proteasomal degradation. This is mediated by the so-called 'β-catenin destruction complex' which is held together by the key scaffolding protein, axin. When present (Wnt on), Wnt ligands bind to Frizzled and LRP6 receptors, resulting in a Dishevelled-dependent oligomerization of LRP6 and its CK1γ/GSK3-mediated phosphorylation. The resulting LRP6 signalosomes sequester Axin thus freeing β-catenin to function with TCF as a transcriptional co-activator of Wnt target genes in the nucleus.

1.6 Diagnosis

Suspicion of classical AC usually arises when adolescents or young adults present with heart palpitations, syncope, or cardiac arrest. Ventricular tachycardia or premature ventricular beats with left bundle branch morphology and T-wave inversion in the V_1 to V_3 leads on a 12-lead electrocardiogram (ECG) are common reasons to suspect AC. Less-common presentations are RV or biventricular heart failure, which can mimic dilated cardiomyopathy.

The major challenge is to distinguish AC from a normal heart with physiological adaptation to hemodynamic overload, such as occurs in athletes, and from so-called disease phenocopies, which include myocarditis, sarcoidosis, idiopathic RV outflow tract tachycardia, and congenital heart disease with RV overload.

No single, gold-standard criterion is sufficiently specific to establish reliably a diagnosis of AC. Multiple parameters are needed, therefore, as included in the original 1994 Task Force diagnostic criteria, which combined multiple sources of diagnostic information, such as familial, electrocardiographic, arrhythmic, morphofunctional, and histopathological findings. Although they provide an extremely useful common approach to clinical diagnosis in index patients, the 1994 criteria have been shown to lack sensitivity for the identification of early or minor phenotypes, particularly in the setting of familial disease.A limitation of the original Task Force criteria was the lack of quantitative cut-off values for accurate grading of RV dilatation and dysfunction, and fibrofatty myocardial replacement.

Diagnosis of AC is challenging because of the broad spectrum of phenotypic variations and often could be performed later the onset of the disease. It relies on a scoring system of “Major” and “Minor” criteria, proposed by Marcus *et al.* in 1994, which consists of a diagnostic algorithm based on structural, functional, and electrophysiological changes typical of the disease (Table 2) [7, 57]. In particular, these clinical criteria comprise six different categories including structural and histological findings, depolarisation and repolarisation abnormalities, arrhythmias, and family history. “Major” and “Minor” criteria were defined for each category. A diagnosis can be made if a patient fulfils **two major** criteria, **one major and two minor** criteria, or **four minor** criteria, all from different categories. It is considered borderline the diagnosis, which satisfy *one major and one*

minor, or *three minor* criteria. The proposed algorithm possesses sensitivity close to 100% and specificity of 91%, but has the disadvantage of creating a group of patients with uncertain diagnosis, which, according to present indications, must be periodically re-evaluated by imaging techniques. These 1994 criteria were found to be highly specific but not sensitive enough. Indeed for many patients at risk a firm diagnosis cannot be reached. To overcome this issue the criteria were modified in 2010 with the inclusion of the results of genetic studies among the diagnostic criteria (Table 2).

Anyway, diagnosis confirmation is often accomplished by invasive procedures such as endomyocardial biopsy [58, 59].

I. Global and/or regional dysfunction and structural alterations	
Major	**Minor**
• Severe dilatation and reduction of RV ejection fraction with little or no LV impairment • Localized RV aneurysms • Severe segmental dilatation of the RV	• Mild global RV dilatation and/or reduced ejection fraction with normal LV. • Mild segmental dilatation of the RV • Regional RV hypokinesis
II. Tissue characterisation of the wall	
Major	**Minor**
Fibrofatty replacement of myocardium on endomyocardial biopsy	
III. Repolarisation abnormalities	
Major	**Minor**
• Inverted T waves in right precordial leads (V1, V2, and V3) • *Epsilon waves in V1 - V3* • *Localized prolongation (>110 ms) of QRS in V1 - V3*	• *Inverted T waves in V2 and V3 in an individual over 12 years old, in the absence of a right bundle branch block (RBBB)*
IV. Arrhythmias	
Major	**Minor**
Nonsustained or sustained ventricular tachycardia of left bundle-branch morphology with superior axis (negative or indeterminate QRS in leads II, III, and aVF and positive in lead aVL).	Nonsustained or sustained ventricular tachycardia of RVOT configuration, LBBB morphology with inferior axis (positive QRS in leads II, III, and aVF and negative in lead aVL) or of unknown axis>500 ventricular extrasystoles per 24h (Holter).

V. Family history	
Major	Minor
AC confirmed in a first-degree relative who meets current Task Force criteria. AC confirmed pathologically at autopsy or surgery in a first-degree relative Identification of a pathogenic mutation * categorized as associated or probably associated with AC in the patient under evaluation.	History of AC in a first-degree relative in whom it is not possible or practical to determine whether the family member meets current Task Force criteria Premature sudden death (<35 years of age) due to suspected AC in a first-degree relative AC confirmed pathologically or by current Task Force criteria in second-degree relative.
VI. Genetics	
Five genes encoding important desmosomal proteins are thought to account for disease in up to 70% of patients. A number of non-desmosomal gene mutations have been associated with AC. The presence of a pathogenic mutation associated or probably associated with AC in an individual with clinical suspicion of the disease.	

Table 2 | 2010 Task Force Criteria for the Diagnosis of AC modified from Marcus et al 2010 [7].

AC, arrhythmogenic right ventricular cardiomyopathy/dysplasia; aVF, augmented voltage unipolar left foot lead; aVL, augmented voltage unipolar left arm lead; BSA, body surface area; ECG, electrocardiogram; LBBB, left bundle branch block; MRI, magnetic resonance imaging; PLAX, parasternal long-axis view; PSAX, parasternal short-axis view; RBBB, right bundle branch block; RV, right ventricular; RVOT, right ventricular outflow tract; SAECG, signal-averaged electrocardiogram.

1.7 New proposed diagnostic criteria

Diagnosis and treatment of AC remain major challenges of modern cardiology.

Novel clinical tools available for the diagnosis of AC include contrast-enhanced cardiac MRI, and electroanatomical mapping.

Cardiac MRI is increasingly used to provide noninvasive tissue characterization of the ventricular myocardium. In addition to identification of RV involvement, this technique can help to identify even early or minor LV involvement, in the absence of morphofunctional abnormalities detected by echocardiography. Electroanatomical mapping can be used to identify the abnormal low-voltage areas, which have been demonstrated consistently in endomyocardial biopsies to correspond with the loss of

electrically active myocardium caused by fibrofatty scarring. Systematic percutaneous catheter mapping of the epicardium in patients with AC in whom endocardial ablation failed confirmed an observation made by pathologists—that fibrofatty replacement (electroanatomical scarring) is more extensive on the epicardial than the endocardial side. However, electroanatomical mapping is invasive and performed only in selected patients with suspected AC and ventricular arrhythmias of RV origin for differential diagnosis with idiopathic RV outflow tract tachycardia, and to guide catheter ablation of the arrhythmogenic substrate.

New diagnostic criteria become necessary: plakoglobin (PG) mislocalization from intercalated disk could represent a good candidate to become a new diagnostic tool [60, 61], but, unfortunately, it presents persisting disadvantages. First of all immunohistochemistry localization can only be performed on bioptic or autoptic samples, and secondary the test is not specific for AC as it is also positive in patients with sarcoidosis and giant cell myocarditis [62].

Non-invasive biomarkers are also actively investigated and BIN1 has recently been proposed as a new circulating biomarker that correlates with HF and predicts arrhythmias in AC patients [63].

Nevertheless the ElectroAnatomic voltage Mapping (EAM) has recently given highly performing results in the setting of suspected AC and of unexplained ventricular arrhythmias. This method shows high sensitivity and sensibility in recognising low-voltage regions, which reflects the fibro-adipose replacement of the myocardium (Figure 6) [64, 65].

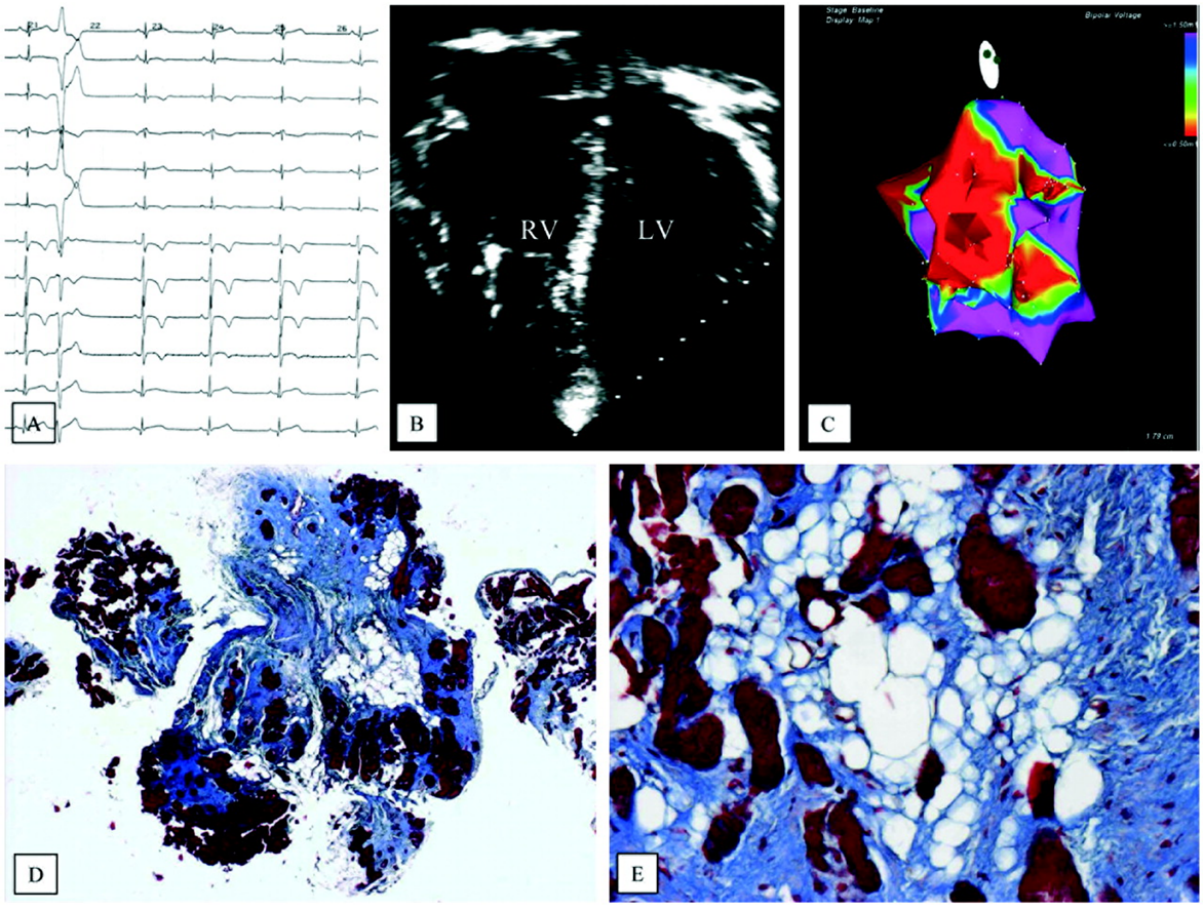

Figure 6 | Noninvasive and invasive findings in a representative patient with abnormal RV electroanatomic voltage map.[66]

A, Twelve-lead ECG showing inverted T waves from V1 to V4 and a premature ventricular beat with a left bundle branch block/superior axis morphology. B, Two-dimensional echocardiographic apical view showing severe RV dilatation. C, Right anterior oblique view of RV bipolar voltage map showing low-voltage values (red indicates <0.5 mV) in anteroinfundibular, inferobasal, and apical regions. D, EMB sample showing massive myocardial atrophy and fibrofatty replacement (trichrome; magnification ×6). E, Close-up showing residual myocytes entrapped within fibrous and fatty tissue (trichrome; magnification ×40).

1.8 Treatment

As the causal mechanisms of AC are poorly understood, it is difficult to define a standard therapeutic approach. The treatment is essentially empiric and based on patient's clinical manifestations, arrhythmic risk and compliance. Every therapeutic methodology has the goal to prevent life-threatening arrhythmias and SCD. A therapy to reverse the fibro-adipose substitution is not available. Possible interventions are lifestyle changes, such as avoiding strenuous exercise, antiarrhythmic drug administration, surgery and placing of an Implantable Cardioverter Defibrillator (ICD). Finally, heart transplantation should be considered in case of patients with progressive HF and refractory recurrent ventricular arrhythmias [67].

Ablation therapy is often carried out during electrophysiological studies, with the aim of destroy areas of re-entry in the myocardium that lead to VTs, by burning the foci of re-entry away. In the same occasion may be done a diagnostic biopsy in order to determine the clinical diagnosis. It may be considered as a possible ICD alternative [68].

Since 1990's, pharmacological treatment for serious arrhythmias has been replaced by ICD implantation. ICD is a battery-operated system that recognizes VTs and VFs and terminates them, preventing SCD. Rare problems occur with ICD, including device failure issues, infections [69] and surgical complications [70].

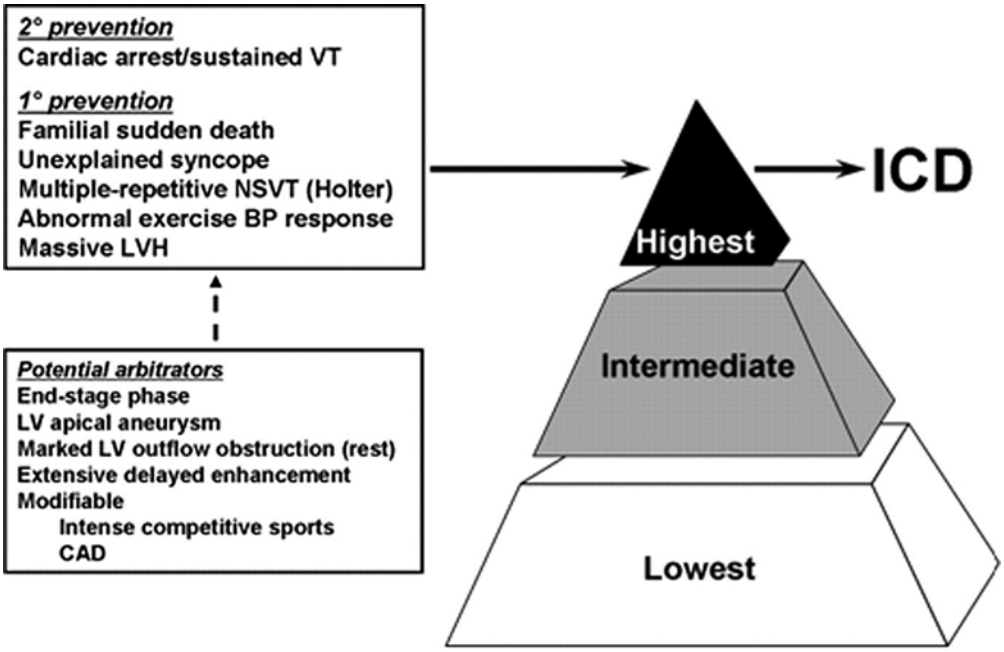

Figure 7 | Stratification risk in SCD prevention and for ICD implant [71].

SCD risk stratification. Top, Pyramid profile currently used to identify those patients at highest risk for SCD who are potential candidates for ICD. BP indicates blood pressure; LVH, LV hypertrophy; NSVT, non-sustained VT. Sustained ventricular tachyarrhythmias have been reported in a significant minority of patients (≈10%) over the short term after alcohol septal ablation. Bottom, Direct relation between magnitude of LV hypertrophy (maximum [max] wall thickness by echocardiography) and SD risk. Mild hypertrophy conveys generally lower risk; extreme hypertrophy (wall thickness ≥30 mm) conveys the highest risk as a marker for SCD.

Clinical studies have identified a number of possible predictors of arrhythmic risk [72-76] such as: aborted sudden death, unexplained syncope and unstable sustained ventricular tachycardia, severe dilation/dysfunction of the right ventricle, left ventricle or both, early onset of the disease, extent of bipolar right ventricle low voltage area, ventricular fibrillation inducibility at programmed electrical stimulation, low Tricuspid Annulus Plane Systolic Excursion (TAPSE).

As for the bi-ventricular structural degeneration, no therapies are present with the exception of heart transplantation in patients with end-stage HF [77].

2. microRNA

2.1 Overview

microRNAs (miRNAs) constitute a large family of 21-25 nucleotides, endogenous, single-stranded RNA molecules [78], evolutionarily conserved among many distantly related species; this suggest that miRNAs play a very important role in essential biological processes.

The first miRNAs (lin-4, let-7) were identified in *C. elegans* (Reinhart, Weinstein et al. 2002) when they were called small temporal RNAs (stRNA). The lin-4 and let-7 stRNAs are now recognized as the founding members of an abundant class of tiny RNAs (e.g. miRNA, siRNA, coRNA, ncRNA) (Figure 8).

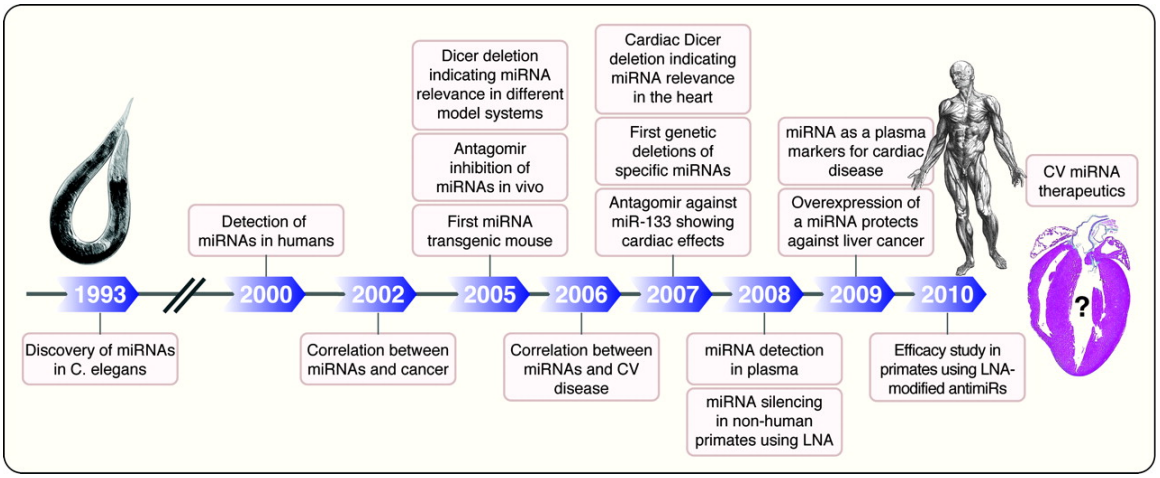

Figure 8 | Breakthrough discoveries in miRNA biology [79].

Time line indicating seminal discoveries in miRNA biology with a special focus on the cardiovascular field.

miRNAs are involved in several biological processes, including development [80], differentiation [81], apoptosis [82] and cell cycle regulation [83]. miRNAs have also recently emerged as key regulators of the networks involved in the Toll Like Receptors signalling pathways where they act as activators of the immune system to provide both host defence against pathogen infections and mediators of an increased metastatic proliferation in tumors [84]

It has been shown that misregulation at any of these processes due to abnormal miRNAs expression or mutations can potentially lead to disease [85] or cancer [86]. Moreover pathological processes can induce the increase or the decrease of some miRNAs, as it occurs in myocardial infarction (MI). In fact, D'Alessandra et al. demonstrated that miR-1, miR-133a, miR-133b and miR-499-5p were highly expressed in MI patients, while mir-122 and miR-375 were reduced [87].

In addition miRNAs have been reported to influence even gene expression by directly binding DNA [88-90] and, at least, some miRNAs can even activate, rather than inhibit gene expression [91].

2.2 Biogenesis

miRNA biogenesis starts with transcription in the nucleus [92] by RNA polymerase II [93] to form primary miRNA transcripts (pri-miRNA) [94].

Many pri-miRNAs are polyadenylated and have a 5' 7-methylguanylate cap [95]. Usually, one miRNA gene codes for a single miRNA, but there are also miRNAs that are clustered together and transcribed as one transcript [96].

A typical human pri-miRNA consists of one or more hairpin structures, and each hairpin has a stem of 33 base-pairs, a terminal loop, and two upstream and downstream single-stranded flanking segments [97].

The pri-miRNA is cleaved by the so called "microprocessor complex" consisting of an RNase III enzyme, Drosha, and the DiGeorge Critical Region 8 (DGCR8) [98].

The product of this cleavage is the precursor miRNA (pre-miRNA), which is approximately 70 bp long, with a 3' overhang of 2 nucleotides, and that is exported from the nucleus to the cytoplasm by Exportin-5 in a RanGTP dependent manner [99]. Exportin-5 recognizes the pre-miRNA and binds properly the pre-miRNA only according its length (minimal 16 bp) and its single-stranded flanking regions [100].

In the cytoplasm another member of the RNase III family, Dicer, cleaves off the pre-miRNA loop and generates an approximately 22-nucleotide miRNA duplex [92], containing the guide strand (mature miRNA) and the passenger strand (miRNA*).

After cleavage, the mature miRNA duplex is loaded into a protein of the Argonaute (Ago) family, usually Argonaute 2 (Ago2), that will in turn recruit the other elements of the RNA-induced silencing complex (RISC). Upon loading, the miRNA* is degraded, while the guide strand will stay tethered to Argonaute and mediate target recognition.

It is believed that from each pre-miRNA, only one of the duplex strands is able to be functionally incorporated into Ago2 [101], while miRNA* is degraded.

As of release 19 of miRBase (http://www.mirbase.org/), all mature forms are now annotated as 5p for the mature form on the 5' arm of the hairpin and 3p for the mature form on the 3' arm of the hairpin, regardless of their relative expression level in the conditions profiled [102].

The canonical mechanism of miRNA-mediated gene regulation occurs at the posttranscriptional level, by targeting the 3' untraslated region (UTR) of an mRNA and inhibiting protein production [103]. miRNAs have also rarely shown to target the 5'UTR and the open reading frame (ORF) binding site to regulate mRNA expression [104, 105].

2.3 Circulating miRNAs

In 2008, two different groups demonstrated that miRNAs are present at detectable levels in humans' serum and plasma [106, 107]. They also illustrated that circulating miRNAs are very stable and could tolerate multiple freeze-thaw cycles, long periods of storage, extreme pH conditions, and showed resistance to RNase A digestion.

Since 2008 has been shown that circulating miRNAs can be packed in exosomes [108], microparticles [109] and bound to high density lipoproteins (HDL) [110] or ribonucleoprotein complexes [111].

2.4 miRNA as biomarkers

Circulating miRNAs retain a number of characteristics that make them ideal biomarkers: stability under various conditions, the possibility to be detected through non-invasive methods, to easily measure them with high sensitivity and specificity using methods among which qRT-PCR is the most used [107]. Since their levels may significantly change upon several stimuli, circulating miRNAs have been proposed as diagnostic biomarkers in different pathologic conditions, such as cancer [112], cardiovascular disease [113], drug induced liver injury [114, 115], diabetes [116], hepatitis [117, 118] and sepsis [119]. The mechanisms underlying miRNAs release into the bloodstream are still unknown and are currently being investigated [120]. Recent reports have described the diagnostic potential of miRNAs in cardiologic diseases such as HF [121], Myocardial Infarction (MI) [87], and Atrial Fibrillation (AF) [122, 123].

3. Cardiac Mesenchymal Stromal Cells (C-MSCs)

3.1 Mesenchymal Stromal Cells (MSCs)

Mesenchymal Stromal Cells (MSCs) are adult, fibroblast-like multipotent cells characterized by the ability to differentiate into tissues of mesodermal origin, such as adipocytes, chondroblasts, osteoblasts [124, 125] and also in endothelial cells, contributing to the revascularization of ischemic tissue. Several studies have shown that both MSCs differentiation in many tissues and their function can lead to the repair of damaged organs and the reconstitution of the immune system. First identified and isolated from the bone marrow (BM-MSCs) can now be expanded from a variety of other tissues including adipose tissue [126], umbilical cord blood, liver [127], skin, tendon, muscle, and dental pulp [128]. MSCs can be isolated based on their ability to adhere to plastic culture dishes, and they are capable of significant expansion by consecutive in vitro passaging [125] of the so-called "colony forming units". They are characterized by the expression of mesenchymal surface antigens such as CD44, CD105, CD29, and CD90. It has been reported that MSCs, in vitro, secrete various bioactive molecules anti-apoptotic, immunomodulatory, angiogenic, anti-scarring, and chemoattractant properties, while, in vivo, interact with immune cells of the innate and adaptive system, in order modulate them [129]. The ability of MSCs to perform all these functions, opened the horizons on their potential use in the clinical setting and in particular in the field of regenerative medicine.

3.2 Cardiac Mesenchymal Stromal Cells (C-MSCs)

In 2010, Rossini et al., firstly identified and characterized a population of cardiac mesenchymal stromal cells (C-MSCs) isolated from adult human auricles [130].

In a normal adult heart, cardiomyocytes represent only 30% of the total cell number. The remaining 70% consists of other cells, among which C-MSCs are the vast majority [131]. C-MSCs play a crucial role in maintaining normal cardiac function, as well as in cardiac remodelling during pathological conditions [132]. In 2015, for the first time Sommariva et al. [133] attribute C-MSCs a role in AC adipose substitution in human hearts. The group

provided evidence that in AC patient's hearts cells differentiating into adipocytes express mesenchymal markers. C-MSCs isolated from human AC hearts express desmosomal genes and are more prone than C-MSCs from control hearts not only to accumulate fat (lipogenesis), but to specifically differentiate into adipocytes. Moreover, C-MSCs exhibit evidence of PG nuclearization and Wnt pathway inhibition [29].

AIMS OF THE STUDY

Diagnosis of AC is challenging because of the broad spectrum of phenotypic variations and often could be performed later than the onset of the disease. Diagnostic criteria follow the Marcus' guidelines[7]: they rely on this scoring system based on "Major" and "Minor" categories. Despite categories specificity, they are not so sensitive in the recognition of AC. In addition, other arrhythmic pathologies, which share AC phenotype, make the diagnosis even more difficult.

Moreover the lack of sensible and specific biomarkers for an early and non-invasive diagnosis, could lead to a not so easy recognition of the early stages of the pathology. Early diagnosis made through a low cost and non-invasive diagnostic test may be life-saving for many AC patients.

At the best of our knowledge no previous studies investigating miRNAs expression/regulation in AC are present in the literature.

This study is focused on the recognition of circulating miRNAs associated with AC, which can be helpful in AC diagnosis and their involvement in the onset and progression of the disease.

In this study we aimed:

1. To screen the level of expression of miRNAs in plasma samples of AC and non-AC male subjects.
2. To assess the specificity of potential miRNAs in diagnosing AC. In particular to identify the differential expression of plasma miRNAs in AC patients vs. healthy controls (HC) and/or patients with ventricular arrhythmias of different aetiologies: idiopathic ventricular arrhythmias (IVT) and patients with ischemic ventricular arrhythmias (IC).
3. To evaluate a possible correlation between miRNAs expression and the severity of the disease in terms of ventricular function and fibro-adipose replacement of the myocardium by means of ElectoAnatomic voltage Mapping [EAM] and Late

Gadolinium Enhancement (LGE) detected by Contrast Enhancement Cardiac Magnetic Resonance (CE-CMR)

4. To assess in cardiac stromal mesenchymal cell cultures how different levels of expression of the identified miRNAs may regulate the onset and progression of the fibro-adipogenesis.

4. Study Population

From September 2014 to September 2015 all consecutive patients referred to our Arrhythmia Center of the Cardiologic Center (Monzino, Milan) because of ventricular arrhythmias were enrolled in the present study.

In the present study a total of 114 male subjects were enrolled: 35 patients affected by AC, 35 were HC, 20 were affected by IVT and 24 were affected by IC.

The overall population was divided in four groups:

Goup A: patient affected by AC with a history of ventricular arrhythmias.

Group B: patients with idiopathic ventricular tachycardia (IVT) (Right or Left Ventricular Outflow Tract tachycardia (RVOT/LVOT).

Group C: patients with ischemic ventricular tachycardia

Group D: healthy controls/donor

Patients were diagnosed with AC according to the International Task Force (ITF) criteria (2 major criteria or 1 major criterion plus 2 minor criteria or 4 minor criteria). Each patient with a suspect diagnosis of AC underwent intracardiac electrophysiological study to assess VT/VF inducibility as well high density EVM.

AC and VT patients were enrolled in the study if satisfying Marcus diagnostic criteria (Marcus, McKenna et al. 2010) and if they were clinically considered affected by Right or Left Ventricular Outflow Tract tachycardia (RVOT/LVOT), respectively.

Once enrolled in the study, from each patient the following data were collected:

- Detailed cardiac evaluation including family history and physical examination
- 12-lead ECG recording
- 24-hour ECG Holter monitoring

- transthoracic echocardiography
- cardiac catheterization including RV and left ventricular (LV) cineangiography in the right and left anterior oblique view
- Coronary angiography
- RV endomiocardial biopsies when indicated
- Blood samplaes for RNA extraction
- Contrast Enahanced Cardiac Magnetic Resonance
- A complete electrophysiological study
- An electroanatomic voltage mapping

Our Ethical Committee approved the study, and all patients gave their written informed consent. Blood samples were collected in basal condition and plasma was obtained by centrifugation, according to the pertinent Italian legislation and Helsinki declaration.

5. Contrast Enhanced Cardiac Magnetic Resonance (CE-CMR)

Each patient underwent Contrast Enhanced Cardiac Magnetic Resonance (CE-CMR).

The exam was performed with a 1.5-T scanner (Discovery MR450, 1.5 Tesla, GE) using a comprehensive dedicated protocol.

The following data were collected:

- RV and LV volumes
- RV and LV function
- Presence and extension of late gadolinium enhancement deposition.
- Presence bulging areas
- Evaluation of RV/LV wall and wall motion abnormalities
- Evaluation of Fatty Infiltration;
- Evaluation of Fibrosis.

The data, including post-contrast sequences, were acquired according to the following CMR study protocol:

1. steady-state free precession sequence (true fast imaging in steady state) cine loops in sequential short-axis views and transverse long-axis views of RVOT;

2. T1-weighted turbo spin-echo images in the axial and short-axis planes;

3. T2-weighted short tau inversion recovery for fat suppression.

4. Ten minutes after administration of contrast agent (gadobenate dimeglumine, Multihance, Bracco, 0.2 mmol/kg of body weight), 2D segmented fast low-angle shot inversion recovery sequences, after at least 10 minutes, were acquired in the same views of cine images, covering the entire RV and LV. Considering the T1 relaxation times of the tissues and the wash-in and wash-out kinetics of extracellular interstitial contrast agents, the optimized T1 nullifies the signal from normal myocardium in the images acquired 10 minutes after contrast medium injection. This allows clear visualization of the DCE areas, defined as a signal intensity at least 400% higher than the signal from normal (remote) myocardium or skeletal muscle.

6. Electrophysiological Study

Before the electrophysiological study, all antiarrhythmic drugs were discontinued to allow a complete wash-out (5 half-lives or 6 weeks for amiodarone). Programmed ventricular stimulation protocol included 3 drive cycle lengths (600, 500, and 400 ms) and 3 ventricular extrastimuli while pacing from 2 RV sites (apex and outflow tract). Programmed ventricular stimulation was considered positive if either a VF or sustained VT (ie, one that lasted ≥30 seconds or required termination because of hemodynamic compromise) was induced. Programmed ventricular stimulation was repeated after intravenous isoproterenol infusion in those patients with effort induced non sustained VT.

7. Electroanatomic Voltage Mapping and Endomiocardial Biopsy

All patients underwent right ventricle (RV) electroanatomic mapping performed with CARTO 4 system (Biosense Webster) during sinus rhythm. At least 150 mapping points were sampled with an irrigated- tip NaviStar catheter (ThermoCool® SmartTouch® Catheter, Biosense Webster). In all patients, we used a catheter with a contact sensor to provide contact information during signal acquisition. A contact of ≥10 g considered adequate. In all patients intracardiac echocardiography (SoundStar 3D ICE, Biosense Webster) was used because to give a preliminary view of anatomy of the ventricles and to

confirm of the adequateness of contact during signal acquisition. During the mapping procedure, we analyzed bipolar electrograms, whereas unipolar map was automatically created and analyzed after the biopsy was taken, and before biopsy report knowledge. Reference values for identifying distribution of the pathological areas was evaluated by dividing RV voltage map into 5 segments, such as outflow,

RV endomyocardial bioptic samples were obtained through the right femoral vein via a disposable bioptome (Bipal, Biosense Webster) introduced into a steerable sheath (Agilis NxT, St. Jude Medical).

The bioptome catheter was always displayed into the CARTO 4 system thanks to the Advanced Catheter Localization technology, that allows the localization of all catheters inside the heart thanks to the measurement of changes in the basal electric range generated by patches initially put on the patient's chest and back.

We were able to visualize the bioptome with the CARTO system by putting a small screw into the adapter of the bioptome's handle and pinching it with a couple of alligator clips, creating an electric dipole. Connecting these electric cables to the CARTO system made the bioptome "visible" as any other electrophysiological catheter. In this way we were able to "triple" check (with fluoroscopy, CARTO system and ICE) the tip of the bioptome before sampling the RV.

An EMB guided by EVM was performed in all patients who had an abnormal bipolar map. In every patient, at least 1 sample was obtained from an area with normal bipolar electrograms and one from an area with pathological bipolar electrograms. In patients with a normal bipolar EVM, biopsies were gained from the mid portion of the right-sided interventricular septum. The sites of biopsy were marked on the map. The sites of biopsy were marked on the map. (Figure 9Figure 8).

The biopsy report was correlated the bipolar and unipolar voltage map at the sampling sites and we matched the EVM results with biopsies.

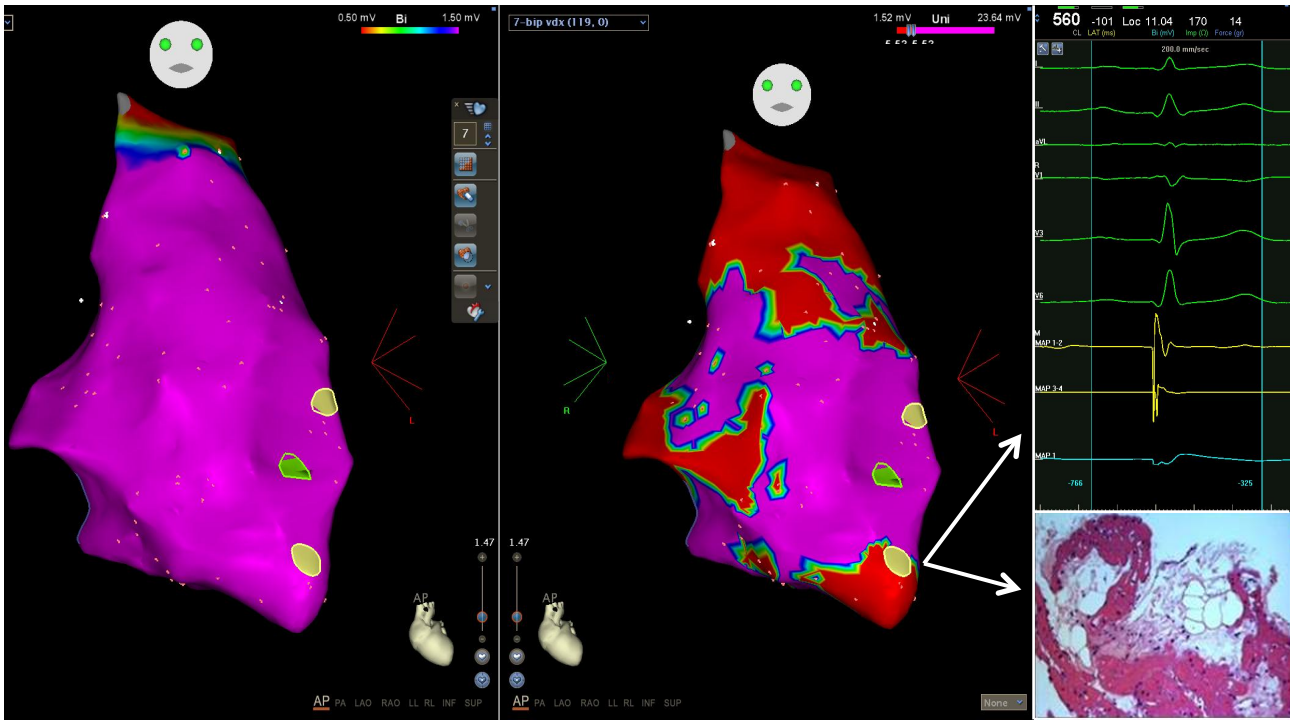

Figure 9 | Electroanatomical Voltage Mapping.

A, Endocardial bipolar voltage map of a patient undergoing endomyocardial biopsy for a suspicion of arrhythmogenic right ven- tricular dysplasia/cardiomyopathy; the map is completely normal. B, Endocardial unipolar voltage map of the same patient; in this case areas of low voltage (red) are evident at right ventricle outflow tract, apex, and peritricuspidalic sites. C, Discordant normal bipolar (yellow) and low-voltage unipolar (light blue) electrograms at withdrawal site. D, The biopsy performed at the apex showed fibrofatty replacement corresponding to 30% of the whole tissue.

8. Histology and Immunohistochemistry Analysis

3 to 4 samples were obtained from each patient for histology and immunohistochemistry analysis.

The analysis were performed by the Cardiovascular Pathology Department of the University of Padova. All samples were fixed in 10% phosphate-buffered formalin and subsequently paraffin enclosed. Serial sections are cut and stained with hematoxylin - eosin and trichrome Azan – Mallory.

Immunohistochemistry for the characterization of inflammatory infiltrates was performed.

1-2 tissue fragments were put into RNA later in order to investigate the presence of viral agents using a molecular biology approach.

In patients presenting histological evidence of fibrofatty replacement, a histomorphometric analysis was performed to calculate the extent of myocardial atrophy and fibrofatty replacement.

9. Plasma samples

Peripheral venous blood samples were collected in 6 ml EDTA-coated VACUTAINER and processed immediately. Cell- and platelet-free plasma was prepared following a two-step centrifugation protocol. Samples were firstly centrifuged at 1.500 × g for 15' at 4°C. The plasma samples, located at the top of the specimen was centrifuged again at 14.000 × g for 15' at 4°C to obtain platelet-poor plasma and, thereafter, divided in 400µl aliquots in 2mL eppendorf tubes and stored at -80°C until use.

10. C-MSCs isolation and culture

Patients with a suspect of AC underwent a series of non-invasive tests and, when needed because of diagnostic confirmation, an endomyocardial biopsy was performed in the area adjacent to the low potential endomyocardial scar and compared to endomyocardial fragments of a group of 5 cadaveric donors with a completely normal heart.

The specimens were washed with phosphate-buffered saline (PBS; Lonza), cut into 2-3 mm3 pieces and incubated at 37°C for 1.5 hours under continuous agitation in Ham's F12 medium containing 3mg/mL collagenase NB 4 (Serva). The digestion solution was then filtered with 70µm mesh nylon filters (BD-biosciences), centrifuged at 400 x g for 10' and the obtained pellet was re-suspended in IMDM medium supplemented with 20% FBS Hyclone (Euroclone), 10ng/ml basic fibroblast growth factor (R&D Systems), 10000 U/ml Penicilin (Invitrogen), 10000 µg/ml Streptomycin (Invitrogen) and 20 mmol/L L-Glutamine (Sigma-Aldrich) (T.MES). Cells were seeded into uncoated Petri dishes (Corning). Non-adherent cells were removed after 24h.

11. Adipogenic differentiation

C-MSCs were cultured in adipogenic induction medium consisting of IMDM supplemented with 10% FBS (Sigma-Aldrich), 0.5 mmol/L 3-isobutyl-1-methylxanthine (IBMX), 1 µmol/L hydrocortisone (HC), and 0.1 mmol/L indomethacin (IM) (Sigma-Aldrich) for 3 and 21 days.

12. Intracellular Lipid Staining by Oil-Red O.

Oil-Red O (ORO) is a fat-soluble dye used for staining of neutral triglycerides and lipids. C-MSC were stained with 1% ORO (Sigma-Aldrich) solution in 60% Isopropanol for 1 hour after 5 minutes fixation with 4% paraformaldehyde in phosphate-buffered saline. Quantitative results were obtained by evaluating luminance of the 255 red channel by ImageJ program (at least 20 fields were evaluated per condition per patient).

Cells were incubated with FITC/PE-conjugated antibodies in 100µl PBS after detachment with 0.02% EDTA solution (Sigma-Aldrich) and analysed with FACSCalibur (BD-Biosciences) flow cytometer. The monoclonal antibodies used in order to confirm mesenchymal lineage and to exclude endothelial and hematopoietic origin are the following: CD44, CD90, CD105, CD29,CD14, CD3, CD146, CD34, CD45. Immunogenicity of the cells was measured through the marker HLA-DR.

Protein	AB	host
CD14	CD14-FITC (MφP9)	Mouse IgG_{2b}, κ
CD29	Integrin β1-PE (clone MAR4)	Mouse IgG_1, κ
CD31	PECAM-1-APC (clone 9G11)	Mouse IgG_1
CD34	Hematopoietic progenitor cell antigen-PE (clone 581)	Mouse IgG_1, κ
CD44	H-CAM-PE (clone G44-26)	Mouse IgG_{2b}, κ
CD45	L-CA-PE (clone HI30)	Mouse IgG_1, κ
CD90	THY1-FITC (clone 5E10)	Mouse IgG_1, κ
CD105	Endoglin-APC (clone 266)	Mouse IgG_1, κ
CD117	c-KIT-APC (clone YB5.B8)	Mouse IgG_1, κ
CD144	VE-Cadherin-APC (clone 123413)	Mouse IgG_{2B}
CD146	MCAM-FITC (clone 128018)	Mouse IgG_1
HLA-DR	HLA-DR-FITC (clone L243)	Mouse IgG_2, κ
KDR	VEGF R2/KDR (clone 89106)	Mouse IgG_1

Table 3 | Lists of antibodies used for FACS analysis.

13. RNA extraction from plasma

Total RNA was extracted from 400 µl of plasma, following a modified TRIzol® protocol for liquid samples.

Samples were thawed, then 1 ml of TRIzol® reagent (Life Technologies) was added and incubated for 5' at RT in order to allow the complete dissociation of the nucleoprotein complex. After adding 200 µl of chloroform for each sample, each tube was mixed by inversion and incubated for 3' at RT. The phase separation was achieved by centrifuging samples at 12,000 x g for 15' at 4°C.

The aqueous phase was transferred to a new tube, where 30 µg of glycogen (Roche) and 1 ml of isopropanol were added in order to induce RNA precipitation. After 10' at room temperature, RNA samples were pelleted 10' at 12,000 × g, washed with 1 ml of ethanol

75%, and centrifuged again 10’ at 12,000 × g. Surnatants were eliminated and, after a 5’ drying step, pellets were resuspended in 52 µl of RNAse-free water.

14. RNA extraction from cells

Total RNA was extracted from pelleted cells with 1 ml of TRIzol® reagent, following the manufacturer’s protocol. Total RNA was resuspended with 32µl of RNase-free water and then quantified.

15. miRNAs screening

TaqMan Human microRNA Card Arrays A&B version 2.0 (Life Technologies) were used for expression screening of 377 miRNAs, conducted on 3 plasma-derived RNA samples randomly selected from AC and 3 gender- and age-matched healty controls (HC).

Reverse transcription (RT) and pre-amplification steps were performed according to the manufacturer’s protocol, using a 7900HT Fast Real-Time PCR System (Life Technologies).

TaqMan MicroRNA Array is an array with 384 wells per card, containing lyophilized primers and probes. The array allows the quantification of the expression of 377 miRNA. 4 small non-coding RNA controls (mammU6), 2 additional endogenous controls, and a sample unrelated with the mammalian species, are respectively used as an internal procedure control and negative control of the card. The 4 replicates of the endogenous control are used to normalize the (Cycle Threshold) Ct values of all 377 miRNAs.

Each card consists of 8 ports, in which 100 µl of sample containing 50 uL of Master Mix, No AmpErase UNG, 49 µl of water Nuclease-free and 1 uL of diluted pre-amplified are loaded. The pre-amplification step is useful to increase the amount of respective cDNA for subsequent PCR Array analysis. The card is centrifuged 2 times, in special adapters, at 1,200 x g for 1 minute. The card is loaded on the instrument 7900 HT Fast Real Time System (Applied Biosystem) for quantitative analysis.

Results were expressed as Ct levels and normalized to the median Ct of each sample (ΔCt), so that all subsequent calculations were independent from the amount of RNA added to the PCR reaction. Relative expression was calculated using the comparative Ct method ($2^{-\Delta\Delta Ct}$). All miRNAs detectable in all 3 samples showing a Ct<30 were

considered as expressed. We considered for the subsequent validation phase only those miRNAs whose expression in AC patients significantly differed from the HC on average more than 2 folds or less than one half.

16. miRNA validation in RNA from plasma and cell samples

All the following steps were conducted by qRT-PCR using single TaqMan microRNA assays (Life Technologies), accordingly to manufacturer's instructions, and calculated as fold change by the 2-ΔΔCt method (ΔCt, ΔΔCt, 2-ΔΔCt).

Since no RNA quantification from plasma sample was possible, the same volume of RNA solution (2 µl) was used in each RT assay for technical consistency.

Conversely, since RNA quantitation from cell sample was possible, RNA samples were diluted in RNAse-free water at the concentration of 2.5 ng/µl in order to use 5ng of RNA solution in each RT assay (2 µl of RNA solution each) for technical consistency.

Profiling data analysis showed 15 potential normalizers that exhibited strong expression in all samples. Among these, miR-210 was identified as the best potential normalizers using the geNorm algorithm. The confirmation step of the screening results was conducted on the same samples used to identify the best internal normalizer, and then the analysis was extended to all remaining samples.

17. Statistical analysis

Quantitative results are expressed as mean ± SD, or mean ± SEM. The analysis of the patients' characteristics was conducted using the Student's T test and the Fisher exact test.

Results obtained with the TaqMan Human microRNA Card Arrays A&B version 2.0 were analysed with Expression Suite v1.0.3 software.

Comparisons of parameters among two groups were made by the unpaired Student's t test. All analysis were performed with 2-tailed t test, considering statistically significant all values of $p < 0.05$ using the Graphpad Prism 5 software.

Regression analysis and ROC curve definition were calculated using the Graphpad Prism 5 software.

RESULTS

18. Patients characteristics

Since Arrhythmogenic Cardiomyopathy (AC) is a rare pathology, which occurs with a prevalence of 3:1 in males, in order to eliminate every confounding variable we decided to analyse only male populations of both patients and healthy controls (HC).

AC patients were enrolled if they fulfilled the Marcus diagnostic Task Force Criteria (two major, one major and two minor, or four minor) (Table 2) [7], using the **following** diagnostic tools. The figures (Fig 10-13) are representative of the results obtained in the patients included in the study for each used diagnostic criteria.

2D-echo, due to its accessibility, low cost and non-invasiveness is one of the first level diagnostic tools and it is able to highlight morphological and functional changes of the heart. In particular we considered both right and left ventricular function as indicated by the values of Tricuspid Annular Plane Sistolic Excursion (TAPSE) and left ventricle Ejection Fraction (EF). Diagnosing AC in patients with minimal right ventricular abnormalities is difficult to accomplish using 2D-echo, therefore it becomes necessary using other diagnostic tools.

ECG interpretation can be helpful in AC recognition. It however rarely represents a diagnostic tool, since AC patients usually have a series of unspecific ECG abnormalities such as T-wave inversion (Figure 10, red arrows), ectopic beats (Figure 10, blue arrows), S wave extension, while the only rare typical ECG abnormality is the presence of ε wave (Figure 10, green arrows).

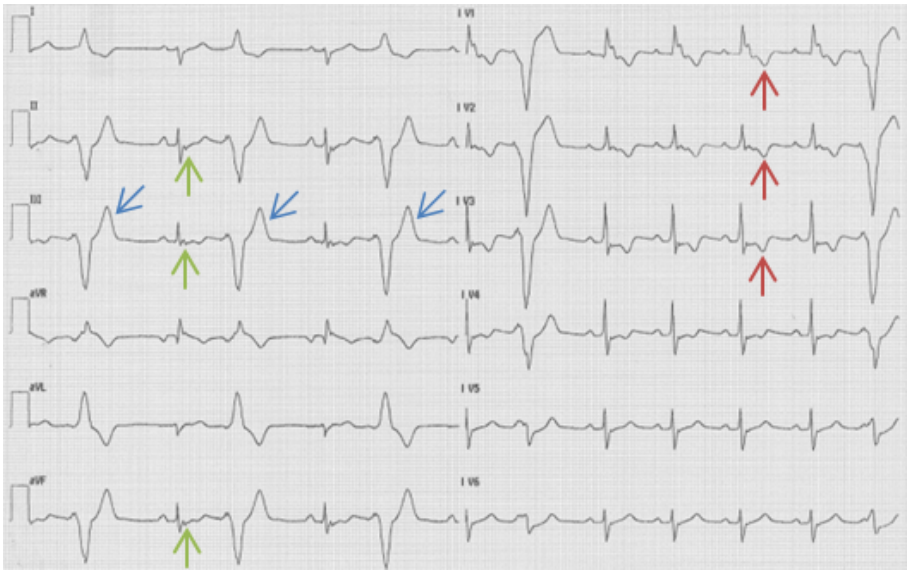

Figure 10 | Typical ECG of a AC patient enrolled in the study.

Green arrows indicate ε wave, blue arrows indicate ectopic beats, red arrows indicate T-wave inversion.

In addition **Holter** monitoring identifies AC rhythm disorders, in which arrhythmias usually originates in the RVOT, showing a Left Bundle Branch Block morphology (LBBB), or from LVOT, with Right Bundle Branch Block (RBBB) morphology.

Furthermore, **Cardiac Magnetic Resonance (CMR)** represents an essential diagnostic tool, due to its accuracy in detecting characteristics cardiac lesions, which cannot be detected with 2D-echo. Indeed, besides dilation, aneurysms formation and alterations in kinetics of the walls of the RV, it can highlight the thinning of the RV wall and its "bulging" areas, characterized by a delay in uptake of the contrast agent (Figure 11, panel A). Though, not considered among the diagnostic criteria, CMR is able to detect adipose infiltration, which appear hyper-intense (Figure 11, panel B). Unfortunately patients with a ICD cannot undergo CMR, thus limiting its diagnostic power.

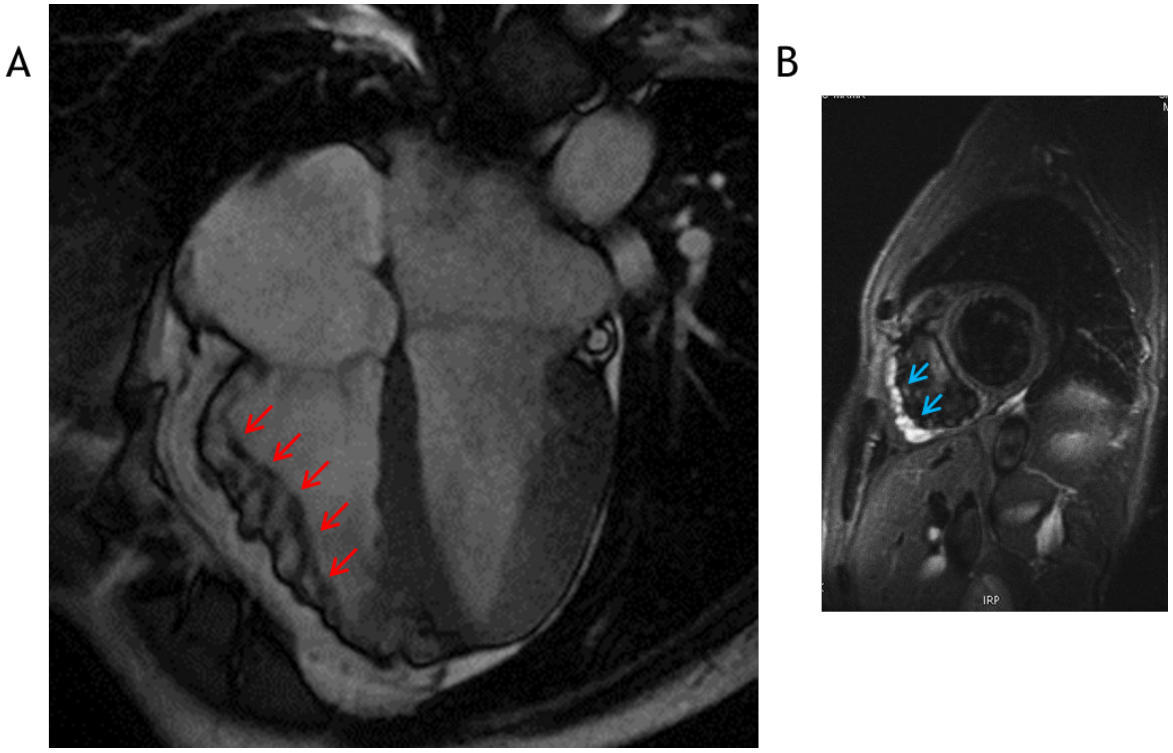

Figure 11 | Typical CMR of a AC patient enrolled in the study.

Red arrows indicate RV bulging, while blue arrows indicate the hyper-intense region, which shows the fibro-adipose replacement of the myocardium.

In certain cases non-invasive diagnostic tools are not sufficient to assess an undeniable diagnosis; therefore it became necessary to perform more invasive procedures. **Electrophysiological Study** tests the inducibility of malignant arrhythmias; **3D-ElectroAnatomic voltage Mapping (**EAM) identifies low-potential areas which reflect scar tissue, that correlate, in AC patients, with fibro- and fibro-adipose replacement of the myocardium [59].

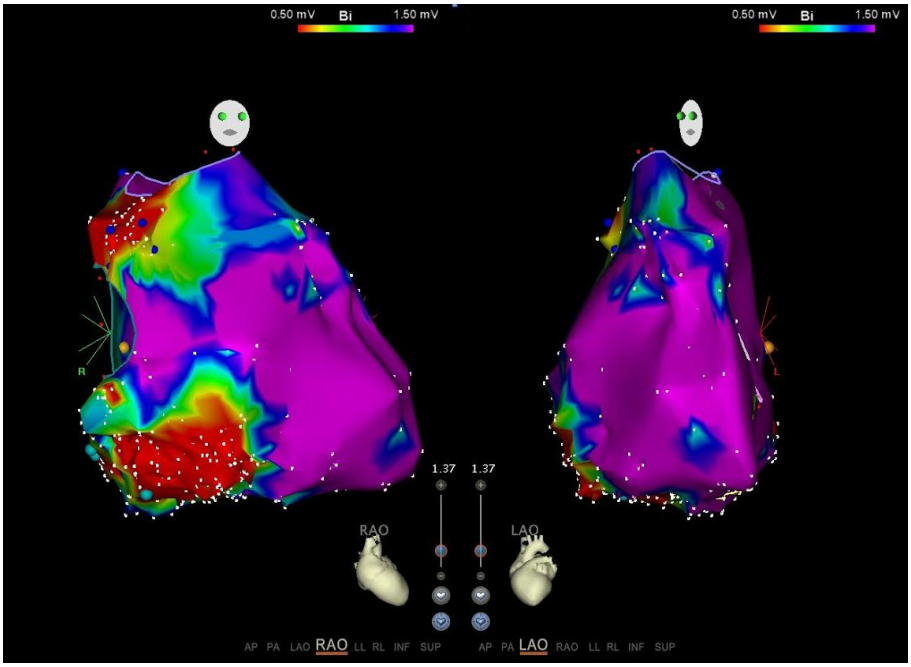

Figure 12 | Example of a Endocardial bipolar voltage mapping of a patient undergoing endomyocardial biopsy for a suspicion of arrhythmogenic cardiomyopathy. Low-voltage areas are represented in red.

EAM is a recognized tool to guide bioptic sampling; **biopsy** is used to perform a quantitative assessment of residual myocardial tissue, cardiomyocytes degeneration and fibro-adipose substitution (Figure 13).

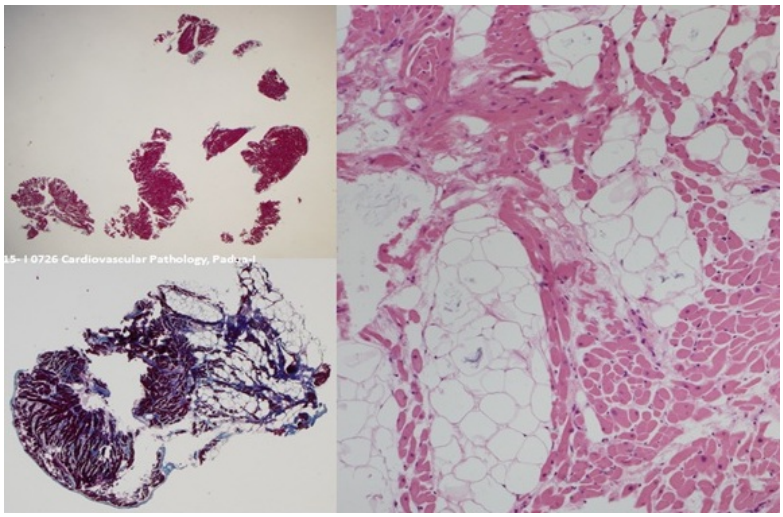

Figure 13 | Example of an endomyocardial biopsy of an our AC patient: histological preparation of a bioptic sample acquired in the pathological area, for diagnostic purposes.

Courtesy of Basso C, Thiene G, Cardiovascular Pathology, University of Padua

Typically, the appearance of signs and symptoms occurs in a sequential manner. In late phases fibro-adipose substitution may proceed to severe RV dysfunction, and further to biventricular heart failure, which, in the worst cases, requires heart transplantation (Figure 14).

Figure 14 | Image of an explanted heart of an AC patient enrolled in the study.

RV wall appears thin and translucent. Adipose substitution is visible and prominent. A high-voltage ICD lead positioned across the tricuspid valve in the right ventricular chamber is shown.

From September 2014 to September 2015 a total of 114 male subjects were enrolled in the study after having signed a written informed consent.

The study population was grouped as follows:

1. 35 AC patients, strictly adherent to the Marcus' Task Force Criteria;
2. 35 male age-matched HC donors.
3. 20 patients affected by idiopathic ventricular tachycardia RVOT/LVOT (IVT), according to the current guidelines.
4. 24 patients affected by ischemic cardiomyopathy and ventricular tachycardia (IC)

Patients	n	Age (mean±sd)	p
AC	35	51±12	ns
IC	24	63±14	ns
IVT	20	47±12	ns
HC	35	47±12	ns

Table 4 - Participants to the study.

Table show all patients and HC which participated to the study. Numbers and ages are represented. A t student test recognized no significant difference between the age distribution.

19. miRNA screening

In order to further improve the diagnostic recognition of AC, we decided to investigate the plasma miRNA signature in our cohorts AC patients.

We firstly conducted a screening of circulating miRNAs on AC and NON-AC plasma samples. In particular the expression of 377 miRNAs in plasma from 3 symptomatic AC patients and 3 age-matched healthy controls (HC) was evaluated using TaqMan Arrays A.

135 miRNAs were found to be expressed in all screened plasma samples ((Figure 15). Comparison of expression between samples was made using global mean normalization. 5 miRNAs resulted differentially expressed in AC vs HC according to empirically set thresholds: fold decrease < 0.5, fold increase > 2 with $p<0.05$ ((Figure 15).

In a further analysis, giving the low number of patient's plasma samples used in the screening, the possible bias of selection of the patients and the relative low number of miRNAs found to be regulated, we decided to include in the validation process the 2 miRNAs (miR-139-5p and miR-15b) whose p value was close to 0.05 ($p=0.058$ and $p=0.067$, respectively) and the miRNAs regulated just behind the threshold of 2 fold increase (1.9 fold) ((Figure 15).

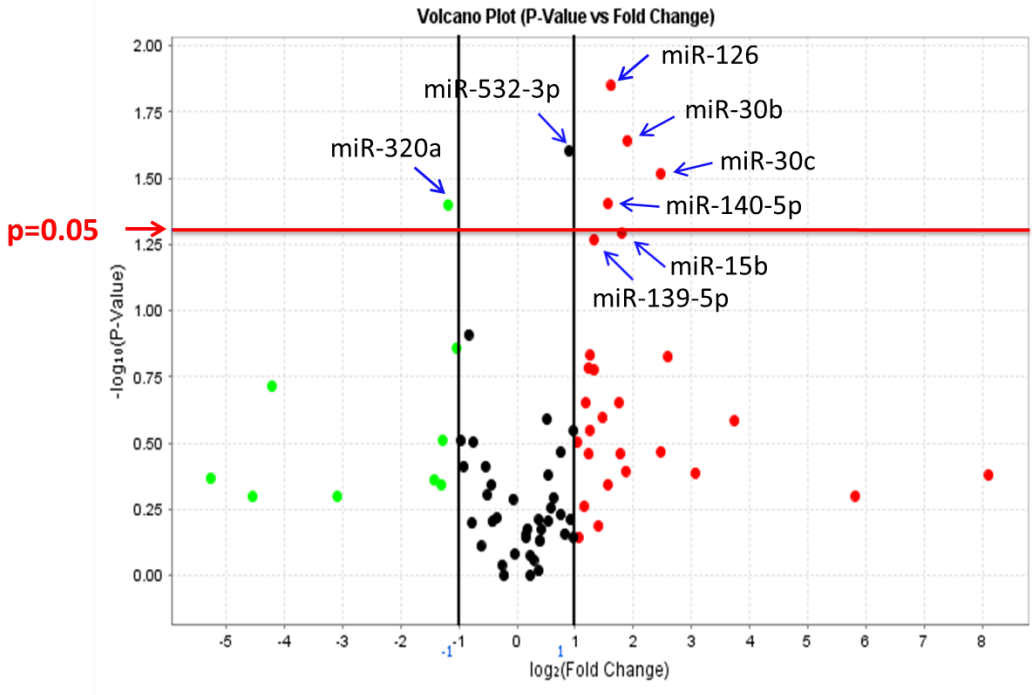

(Figure 15 | Volcano plot illustrating miRNAs potentially regulated after TaqMan Card Array.

Volcano plot shows Taqman Array results. In the graph are represented all dots indicating the fold value of each miRNA. Dots indicated with blue arrows were further tested in the validation step. Red line indicate the minimum significance considered (p=0.05).

20. miRNA validation

The potentially identified miRNAs (miR-320a, miR-532-3p, miR-126, miR-30b, miR-30c, miR-140-5p, miR-139-5p and miR-15b) were subsequently tested by single qRT-PCR in the plasma of a second cohort of 18 patients (9 patients with AC and 9 HC) in order to validate the previous results and to identify which miRNAs might be used as normalizers.

miR-210 demonstrated a strong and stable expression in both groups and therefore was chosen as normalizer. ((Figure 15).

miR-532-3p, miR-126, miR-30b, miR-30c, miR-140-5p, miR-139-5p and miR-15b did not show a statistically significant differential expression between the two groups.

miR-320a was significantly less expressed in plasma samples of AC patients compared to HC.

Then, we evaluated the miRNA-320a expression in the AC patients and age-matched HC-cohort (n=35 each) (Figure 16, panel A). miR-320a expression resulted variably distributed in HC (Figure 16, panel B) and significantly down-regulated in AC patients, with a 0.39 ± 0.02 fold decrease; (p= 0.003) (Figure 16, panel A).

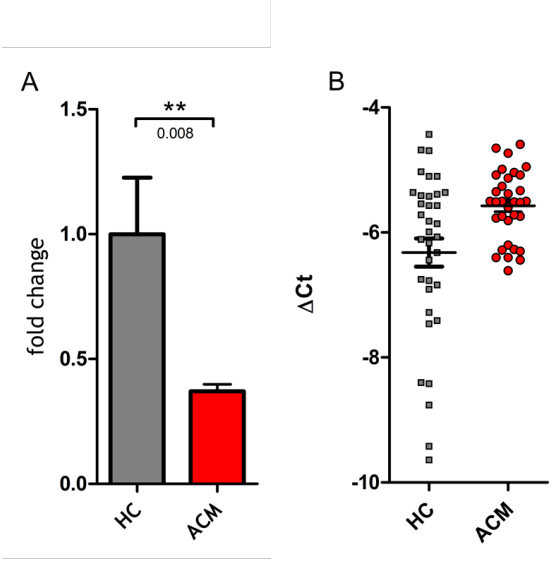

Figure 16 | miR-320a expression in AC patients vs. HC.

Panel A: miR-320a expression in 35 AC patients (red column) vs. 35 HC (grey column), expressed as fold change, black stars represent p values<0.01; panel B: dispersion of ΔCt values in HC (grey squares) vs AC patients (red dots.).

21. miR-320a accuracy

In order to evaluate the accuracy of miR-320a to discriminate AC patients from HC we performed Receiver Operating Characteristic (ROC) curve analysis (Figure 17).

The ROC curve is a tool for diagnostic test evaluation, because it helps to evaluate the accuracy of a test in discriminating the presence of the disease from the lack of the disease in the examinated cases. In a ROC curve the true positive rate (Sensitivity) is plotted as a function of the false positive rate (100-Specificity) for different points of a parameter. In our case, each point on the ROC curve represents a sensitivity/specificity pair corresponding to miR-320a ΔCt values (AC patients vs. HC). The area under the ROC curve (AUC) is a measure of how well a parameter can distinguish between the two diagnostic groups (AC vs. HC). ROC analysis showed an AUC value of 0.77 (p=0.03), indicating a good accuracy of miR-320a as a potential discriminating marker of the diagnosis of AC.

Data analysis showed, for instance, that for ΔCt values of <-5.55 AC diagnosis has 65% of sensitivity and 80% of specificity.

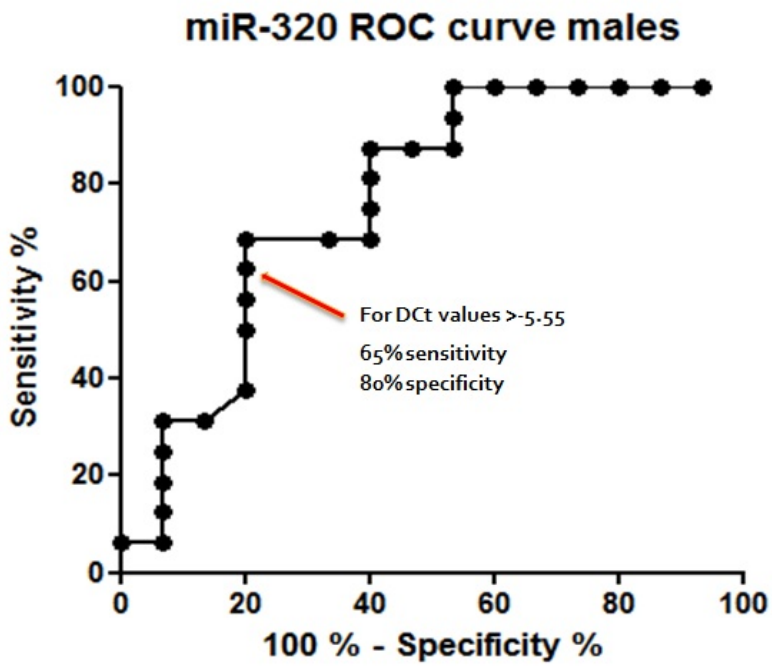

Figure 17 | ROC curve, representing the accuracy of miR-320a in detecting AC patients.

Sensitivity and specificity are plotted for each ΔCt value. ROC curve shows a significant AUC of 0.77 ($p<0.05$).

22. miR-320a in other arrhythmias

In addition, to evaluate whether the lower expression of miR-320a in AC patients was specific of this disease, we decided to investigate if the same findings were present in other arrhythmic disease.

Therefore in order to exclude that miR-320a regulation was associated to unspecific ventricular arrhythmogenic phenotype, its expression was tested in patients with idiopathic ventricular tachycardias (IVT) (n=20), a disease which could be considered in differential diagnosis with AC, and it is characterized by arrhythmias originating often within the same anatomical site as AC but with different underlying pathophysiological processes. Also a group of patients affected by ischemic ventricular arrhythmias (IC) (n=24) was included in the study.

MiR-320a was equally expressed in patients with IVT, IC and HC (fold change 1.09±0.15, p=ns; fold change 0.74±0.22, p=ns) but once again was statistically more expressed in patients with IVT compared to AC (fold change 2.79±0.26, p<0.001) (Figure 18).

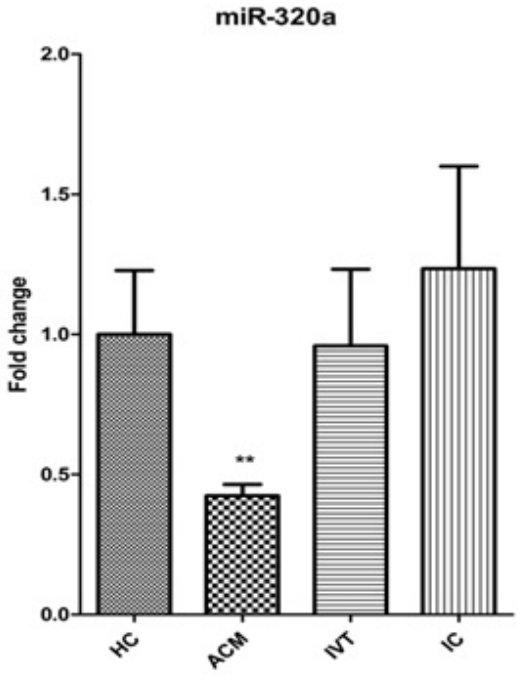

Figure 18 | miR-320a is downregulated only in AC.

*Fold change in miR-320a expression in all populations participating in the study: 35 HC, 35 AC, 20 IVT and 25 IC plasma samples. Black stars represent p values respect to HC (**=p<0.01).*

ROC curve analysis demonstrated a good accuracy of miR-320-a as a circulating biomarker to distinguish patients with ventricular tachycardia affected by Arrhythmogenic Cardiomyopathy and patients with Idiopathic Ventricular Tachycardia (Figure 19).

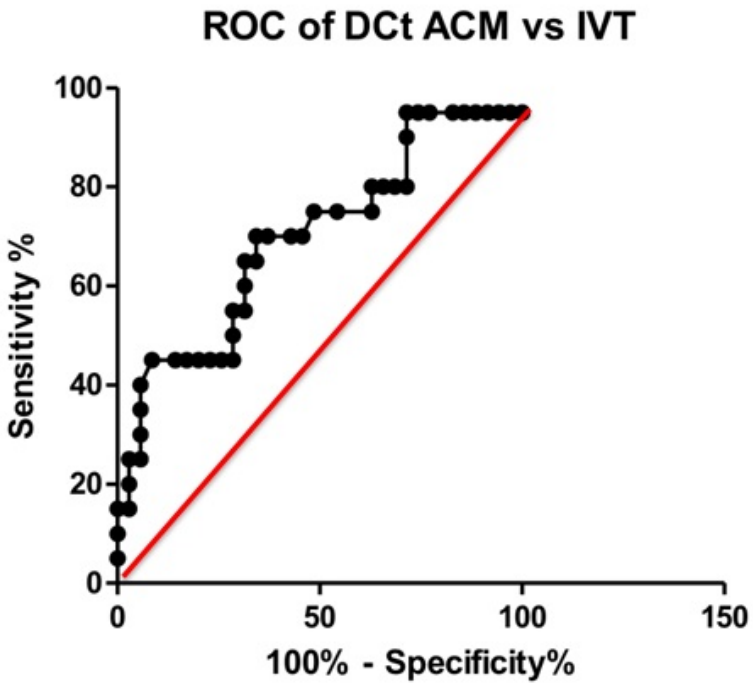

Figure 19 | ROC curve analysis for accuracy of miR-320-a.

23. Correlations between miR-320a and disease severity

We hypothesised that miR-320a expression could be associated with clinical signs of AC severity. We performed the evaluation of the occurrence of major arrhythmic events (MAE) and the semi-quantitative assessment of the functionality of the left and right ventricle, measured with ejection fraction (EF) and Tricuspid Annular Plane Systolic Excursion (TAPSE), respectively. Further investigations about the role of the currently use drug therapies allowed us to conclude that the presence of antiarrhythmic therapies did not influence miR-320a expression.

As shown in Figure 20 we observed a significant correlation (r^2=0.20 p<0.04) between impairment of LV function and ΔCt expression: patients with a lower expression of miR-320a showed a greater impairment in EF.

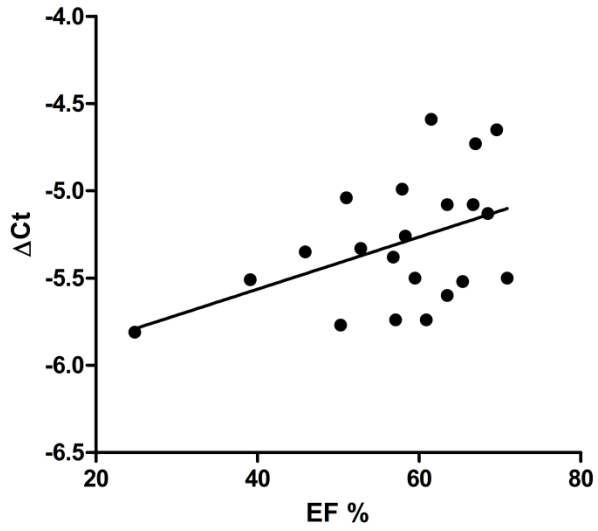

Figure 20 | Linear regression of ΔCt vs. EF percentage values in AC patients.

The regression line represents the interpolation between miR-320a ΔCt values and left-EF percentage. Dots represent single values per AC patient.

Moreover, as shown in Figure 21 a similar, even not-significant trend (r^2=0.12; p=0,08), was observed in the correlation between TAPSE impairment and miR-320a ΔCt.

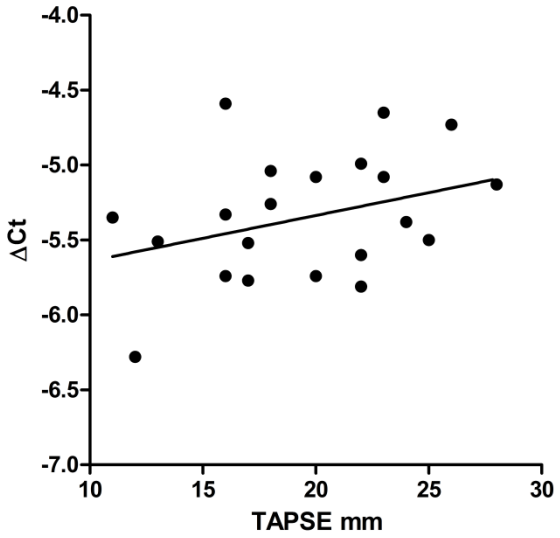

Figure 21 | Linear regression of ΔCt vs. TAPSE values (mm) in AC patients.

The regression line represents the interpolation between miR-320a ΔCt values and TAPSE percentage. Dots represent single values per AC patient.

We then evaluate miR-320a plasma expression and its possible correlation with areas of scar (percentage of LGE) into the right/left ventricle, calculated by CMR in 12 AC patients.

As seen in Figure 22 we observed that fibro-adipose progression could be linked with miR-320a expression even if the simple regression analysis did not result in a statistical correlation (r^2 value 0.26 and p=0.08).

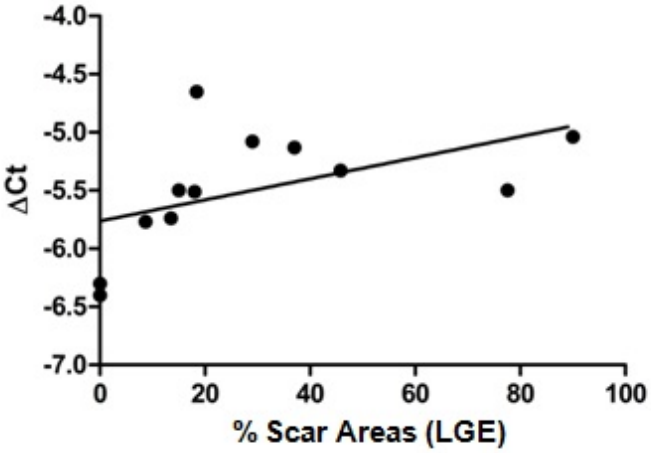

Figure 22 | Correlation between miR-320a expression (ΔCt) and scar areas obtained at the CMR obtained.

The regression line represents the interpolation between miR-320a ΔCt values and scar areas. Dots represent single values per AC patient.

In addition we analysed mir-320a expression and the presence of scar at CMR and EAM low-voltage areas obtained in the RV/LV with CARTO system in AC patients.

The correlation between miR-320a expression (ΔCt) and unipolar scar areas obtained with EAM despite not statistically associated, showed a common trend (p=0.07). (Figure 23).

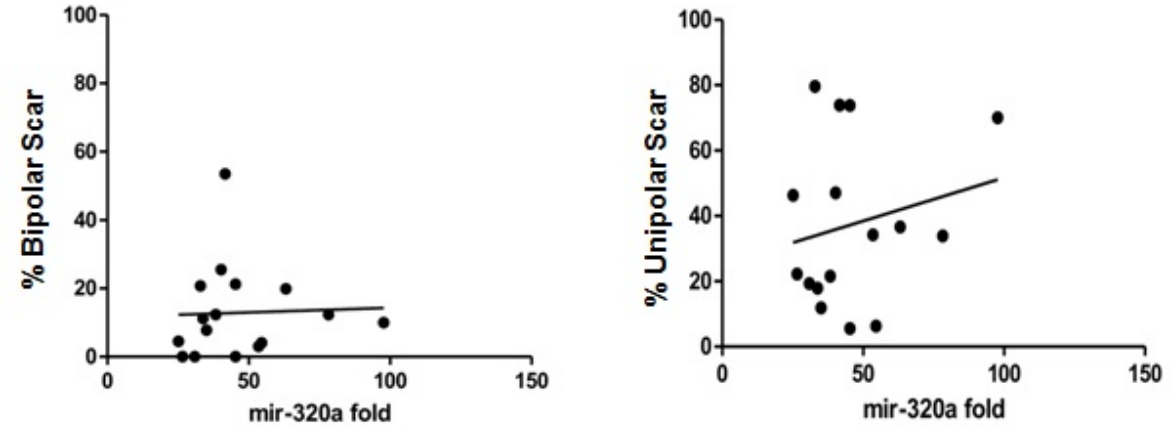

Figure 23 | Correlation between miR-320a expression (ΔCt) and scar areas obtained at the EAM obtained (bipolar and unipolar voltage mapping).

24. miR-320a characterisation

It has been demonstrated that miR-320a, in prostate cancer, inhibited Wnt/β-catenin signalling pathway by targeting the 3'-UTR of β-catenin mRNA [134]. Wnt pathway is involved in AC pathogenesis [29], adipogenic differentiation [135] and it is regulated in human mesenchymal stromal cells [136]. In addition it was recently published that human skeletal-MSCs undergo adipogenic differentiation through a mechanism involving miR-320 family [137]. According to these literature data, we speculate that the lower plasmatic expression of miR-320a we observed in AC patients may correlate with the adipose substitution in AC hearts.

25. Cardiac Mesenchymal Stromal Cells in AC

Since Cardiac Mesenchymal Stromal Cells (C-MSCs) from AC ventricular samples have been obtained in our laboratory and have been used as *in vitro* model of AC, we decided to evaluate miR-320a in this model.

C-MSC primary lines of AC (n=6) and NON-AC (n=5) were available for *in vitro* study.

To characterize the immunophenotype of C-MSCs, different plasma membrane domains (CD) were assessed to exclude hematopoietic and endothelial lineage origin and confirm therefore their mesenchymal characteristics of the obtained cells.

As shown in Table 5 our cells are of mesenchymal origin, they show low presence of CD31. The expression of the hematopoietic markers CD34 and CD45 was absent.

	ACM (n=6)	NON-ACM (n=5)	p
CD29	96.17±0.97	98.64±0.31	ns
CD105	93.44±2.52	96.38±1.32	ns
CD44	93.80±2.31	98.29±0.41	ns
CD90	34.45±12.12	6.98±2.69	ns
CD31	4.50±3.41	4.46±4.23	ns
CD34	0±0.54	0.98±0.76	ns
CD14	1.65±1.20	0±0.40	ns
CD45	0±0.58	0.07±0.76	ns
CD117	1.29±0.19	1.24±0.39	ns
HLA-DR	0.29±0.38	0.11±0.24	ns

Table 5 | Detailed FACS analysis of AC and NON-AC C-MSCs.

All FACS antibodies used for the immunophenotype analysis. AC and NON-AC colum represent the mean percentage±standard error of positive cells to the specific antigen.

As shown both in Table 5 and Figure 24 our AC C-MSCs are similar to NON-AC cells concerning both composition and morphology. CD90 is poorly expressed in our cells, as already described for mesenchymal cells of non-bone marrow origin [138], but it is a little more expressed in AC cells than in controls, as expected in cells obtained from a more fibrous and fibro-adipose tissue [139, 140].

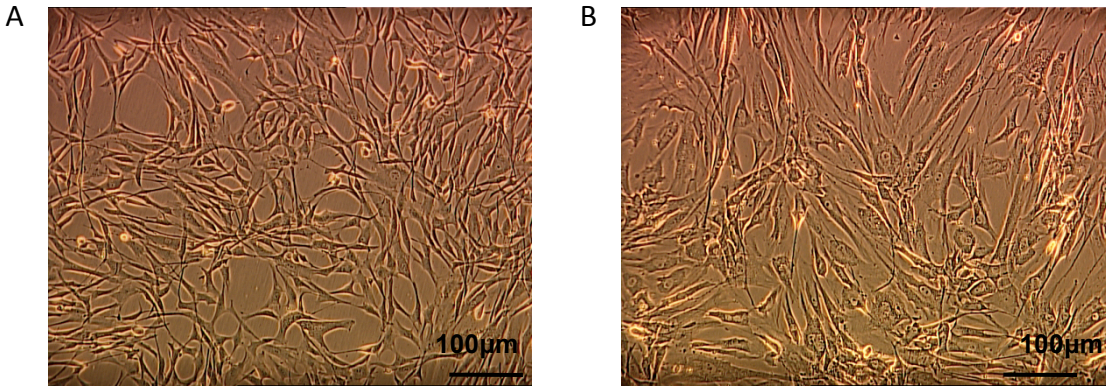

Figure 24 | Representative image of C-MSCs in basal medium (T.MES) (bright field).

Panel A: NON-AC patient-derived C-MSCs; panel B: AC patient-derived C-MSCs.

25.1 C-MSCs during adipogenesis

In order to assess C-MSCs involvement during adipogenesis we planned an *in vitro* experiment in order to attempt to differentiate C-MSCs in to fully differentiated adipocytes thus mimicking what we are hypothesized to happen in the AC development.

We maintained the same plated number of C-MSCs in adipogenic medium for 3 days.

As shown with the ORO staining in Figure 25, panel A and B AC patients-derived C-MSCs (n=6) accumulate more lipid droplets than NON-AC patients-derived C-MSCs (n=5). In addition the quantification of lipid staining measured through the red (255) luminance with ImageJ software showed a statistically significant increase ORO staining in AC cells compared to NON-AC (p=0.004).

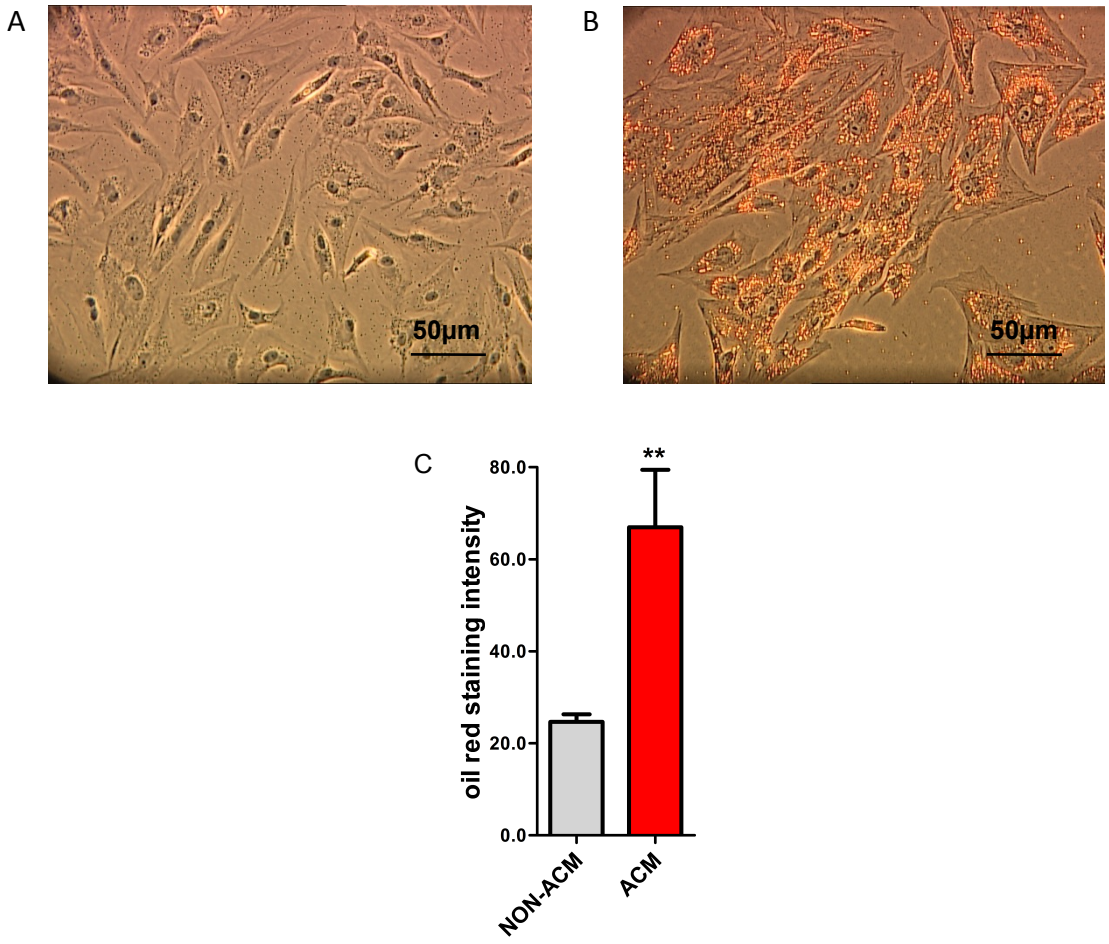

Figure 25 | Representative image of C-MSCs in adipogenic medium (T.ADIPO) after ORO staining (bright field).

Panel A: NON-AC patient-derived C-MSCs; panel B: AC patient-derived C-MSCs; panel C:quantification of ORO staining in NON-AC patient-derived C-MSCs (grey column) vs AC patient-derived C-MSCs (red column).

25.2 miR-320a during adipogenesis in C-MSCs

We planned an *in vitro* experiment to simulate AC development and monitor miR-320a expression in the following two conditions:

1) Basal condition, in which cells were maintained in basal medium (T.MES) for 72 hours;
2) Adipogenic condition, in which cells were maintained in adipogenic medium (T.ADIPO) for 21 days.

As shown in Figure 26, panel A AC C-MSCs showed a lower miR-320a expression, of 0.44±0.08 fold, compared to NON-AC, even if not reaching the statistical significance. Instead, after 21 days of adipogenic induction, we observed that miR-320a is present homogeneously in the two populations, as seen in Figure 26, panel B (1.0 ± 0.11 in NON-AMC and 0.97 ± 0.06 in AC). Panel A and B show the expression of miR-320a in AC cells relative to the NON-AC controls, normalized to 1 to better show the difference between AC and NON-AC samples. In Figure 26, panel C the same raw data, not normalized are plotted as ΔCt, representing the miR-320a expression values, in the two conditions: miR-320a expression in C-MSCs at basal level and after 21 days of adipogenic treatment. Here we evaluated the change in miR-320a levels during adipogenesis for each group. We observed that both groups showed an increase in the miRNA levels during adipogenesis, even if more consistent in AC C-MSCs.

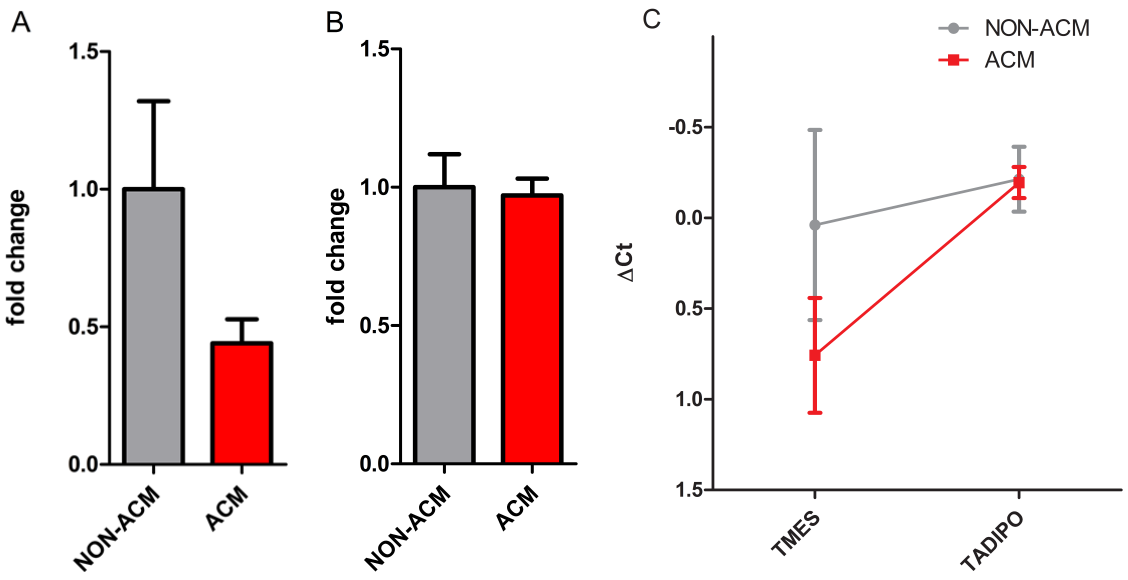

Figure 26 | miR-320a expression during adipogenesis.

Panel A: fold change in miR-320a expression in 5 NON-AC C-MSCs (grey column) vs. 6 AC C-MSCs (red column) at basal condition (T.MES). Panel B: fold change in miR-320a expression in 5 NON-AC C-MSCs (grey column) vs. 6 AC C-MSCs (red column) after adipogenic differentiation (T.ADIPO). Panel C: miR-320a ΔCt (miR-320a Ct – miR-210 Ct values) variation in 5 NON-AC C-MSCs (grey line) vs. 6 AC C-MSCs (red line) at basal condition (T.MES) and after 21d adipogenic differentiation (T.ADIPO). The graph represents the reverse ΔCt values for the two conditions, since lower ΔCt values correspond to higher miR-320a expression.

All the experiments were performed in duplicate.

DISCUSSION

Arrhythmogenic Cardiomyopathy (AC) is a rare pathology, which affects mainly young and athletes, leading to ventricular tachyarrhythmia, right and/or biventricular impairment and in the worst case to Sudden Cardiac Death (SCD).

Clinical diagnosis remains challenging because of its great variability in phenotypic manifestations, incomplete penetrance, and age-related progression. Mainly at its exordium, AC is characterized by a "concealed phase", in which ventricular arrhythmias and SCD are not infrequent, even without overt manifestation of the disease.

Diagnosis is based on a scoring algorithm based on electrophysiological, morphologic and genetic parameters that often does not allow to reach a clear diagnosis leaving high-risk patients to cope with an unsolved issue.

Data obtained during the past year represents a proof of concept aiming to identify an early and non-invasive biomarker for the diagnosis of AC and the preliminary data obtained from cellular model may represents basis for future mechanistic studies in AC pathogenesis.

Thus, a successful early diagnosis, prevention of the deadly complications and the therapeutic approach for this disease depends heavily on the clinical biomarkers for early detection of the presence and progression of the disease, as well as the prediction after the clinical intervention. However, the current clinical biomarkers do not allow to specifically distinguish between those patients who will develop the more aggressive form of the disease and those who should avoid overtreatment for less severe forms enabling physicians to tailor treatment for individual patients. Recently, some researchers have demonstrated that plasma miRNAs are sensitive and specific biomarkers of various diseases. The primary aim of the study was to investigate whether miRNAs present in the plasma of AC patients can be used as diagnostic and prognostic biomarkers.

After an initial screening of 367miRNAs we identified 135 miRNAs differentially expressed in the two cohorts (AC and HC). In miRNA microarray data analysis, the main interest is usually focused on whether a specific miRNA or a set of miRNAs is differentially expressed

in the different sample populations. In order to identify which of the 135 miRNA could be involved in AC, we initially set the following cut-off: the miRNA should have at least a two-fold change in expression and has to have a statistically different expression in the two groups of patients. Since we initially performed this test only in six patients, to avoid any bias related to the small sample, we included in the validation process miRNAs that, at the Volcano plot, localized close to the set threshold.

Because the amount of miRNA in plasma samples is too low to be quantified by traditional methods, all results need to be compared to an internal standard. From the data obtained from the Taqman card array we were also able to identify which miRNAs were potentially equally expressed in the two cohorts. Testing these miRNAs by single miRNA qRT-PCR we were able to identify and validate them as normalizers. Among 15 miRNAs equally expressed in the two groups of patients, miR-210 was chosen given its high expression and its homogeneous Ct distribution in both groups. Normalization is an essential step in microarray gene-expression data analysis. It helps to reduce non-biological errors and to convert raw data to valid results. In particular the choice of normalizers is an important debated issue in the field of plasma screening: one of the challenges of plasmatic miRNAs profiling is the discovery of an established housekeeping genes for data normalization. Another common approach to this purpose is to add exogenous synthetic miRNA mimics (e.g. synthetic *C. elegans* miRNAs that do not have homologous sequences in humans), in plasma samples, before RNA extraction as normalizer. Anyway, despite the use of a fixed plasma volume, this method does not consider that RNA amount may be variable in different samples. Further, it is well known in literature that exogenous miRNAs are not so stable as endogenous ones and they may be degraded, modifying expected results. Therefore, adding a fixed amount of one or several synthetic miRNAs into samples containing variable amounts of RNA for normalizing with qRT-PCR is not the best choice.

Among the 8 miRNAs initially identified because they were differently expressed between AC and HC, only miR-320a overcame the validation process, performed via single miRNA qRT-PCR in plasma of additional 6 AC compared with 6 age-matched HC.

In order to further validate the role miR-320a as a putative biomarker of this rare disease it was assayed in plasma samples coming from a remarkable large population of AC patients (n=35). Validation data were confirmed as seen in Figure 16, panel A

In our selected cohort of AC patients, compared to HC, miR-320a showed a 61% reduction of its expression that we found to be statistically significant, indicating a strong correlation between miR-320a and AC occurrence.

A significant reduction (61%) in miR-320a expression was found in our selected cohort of AC patients when compared to HC, suggesting a strong correlation between miR-320a expression and the occurrence of AC. Despite these important findings, we were aware that a comparison with a population of HC could have been considered an intrinsic limitation of the study with a weakening effect on the relative conclusions. In fact in the everyday clinical setting, when we suspect AC could affect a patient, the differential diagnosis should be made with other conditions leading to ventricular arrhythmias like IVT. In order to avoid this selection bias concerning the reference population we decided to recruit NON-AC and NON-HC patients and in particular we obtained plasma samples of patients affected by idiopathic ventricular tachycardia (VT). By testing miR-320a expression in this population we aimed to further confirm its specificity in diagnosis AC and therefore its possible clinical utility. IVT and HC patients had a very similar miR-320a plasma levels, further enforcing the hypothesis that miR-320a could play a role in AC development.

After having identified miR-320a as a diagnostic tool for AC diagnosis, we tried to investigate its role as a tool for risk stratification. First of all we did not find any correlation between the level of miR-320a expression and any anti-arrhythmic drug taken from the patients, thus excluding them as confounding variables.

Unfortunately we did not find any significant correlation between miR-320a expression and right ventricular function measured by TAPSE, but a slightly significant correlation with left ventricular EF. Unexpectedly, lower EF (meaning a greater left ventricle damage) was associated with higher miR-320a expression, similar to what was found in HC. On the contrary of what we have found we were expecting an inverse correlation: the lower miR-320a levels were the worse the patient's phenotype should be. Anyway, more data are needed to confirm these results and to explain them.

miR-320a expression and AC severity was further evaluated by EAM. As previously described RV EAM is representative of fibro-adipose substitution in AC patients. [64, 65]

We observed that miR-320a slightly correlate with low-potential scar areas, in particular in the unipolar voltage mapping. Indeed, patients with higher miR-320a expression showed small low-potential scar areas; on the contrary, patients with lower miR-320a expression showed greater low-potential scar areas. It is intriguing that a miRNA involved in adipogenic differentiation seems to go along with the adipose scar in AC patients' hearts. Enlarging our cohort, we may be able to offer a new tool to evaluate adipogenic progression in patients' hearts.

Plasma biomarkers are actively investigated because of their non-invasiveness: recently, BIN1 has been proposed as a new circulating biomarker that correlates with HF and predicts arrhythmias in AC patients [63]. Despite its high accuracy in detecting arrhythmic events and in identifying the worst AC phenotype, it has only been evaluated in AC group and not in patients affected by other pathologies; therefore it cannot be considered specific for AC. Since BIN1 recognized HF, it might only correlate with cardiac functional status, independently from AC. A cohort of NON-AC HF patients would be needed to confirm BIN1 as an AC-specific biomarker. It would be interesting to evaluate possible correlation between miR-320a and BIN1 or to combine the two circulating molecules in order to get an AC-specific patients risk stratification.

Beside our AC patients' male cohort we had the chance to consider only 5 women clinically affected by AC, according with the higher male prevalence between patients hospitalized at CCM, than described in literature[18]: indeed we observed a male:female ratio of 6.6:1. We evaluated miR-320a expression in their plasma samples coming from 5 women affected by AC and in 4 age-matched female HC. AC women showed a slightly augmented miR-320a expression compared to HC. Noteworthy, this result showed an opposite trend compared to what observed in male patients. Anyway, this preliminary data, far to be conclusive, has to be considered strongly promising supporting the choice to enlarge the sample size. Intriguingly, software like TargetScan revealed that miR-320a might bind the estrogen-related receptor gamma, constituting an idea for future mechanistic studies to explain higher male prevalence. Future studies are needed to prove this hypothesis.

The link between AC and physical exercise is still unclear. For many AC patients exercise may be the cause of arrhythmias [141]. Several reports also show the occurrence of SCD during physical exertion [142]. Recently literature even focused on a new phenology of AC named exercise-induced AC [143, 144]. Most of the recruited patients (28/33) were athletes or former-athletes, suggesting a possible role of training in predisposing to a worst clinical manifestation. It would be very interesting to evaluate, in the future, miR-320a expression in a cohort of endurance or resistance athletes assessing the independency of our findings from strong physical activity. Additionally, it would be very helpful to compare 2D-echo data of this cohort in order to assess any possible correlation with ventricular functionality and exercise-induced remodeling of the heart.

Our AC cohort, as described in literature, showed a great genotypic heterogeneity. Genetic analysis revealed private mutations in different desmosomal genes (e.g. PKP2 is the most common mutated gene). The evaluation of possible correlations between patients carrying mutations in the same gene and miR-320a expression could be very interesting to study. It may lead to further understand miR-320a involvement in AC development. Moreover, a highly variable penetrance was found in several families with an AC family history. Despite the inheritance of the same mutation AC manifestations are variable and does not depend only on the genetic deficiencies; it would be very interesting to evaluate miR-320a plasmatic levels in our “AC families”, comparing affected individuals to non-affected relatives, carrying the same genetic mutation.

The most intriguing hypothesis coming from our data was the putative effect of miR-320a in the heart tissue derangement in AC and in particular the replacement of the heart tissue with fat. Recent studies have demonstrated that microRNAs are also involved in adipocyte differentiation. *In vivo* and *in vitro* studies have revealed that various microRNAs affect adipogenesis by targeting several adipogenic transcription factors and key signaling molecules.

miR-320a in particular was recently reported to be involvement in adipogenesis [145] so we looked at miR-320a expression in a cellular model of AC adipogenesis. C-MSCs, primary cells, directly obtained from AC ventricular bioptic samples, recapitulate in vitro AC pathogenesis (including Wnt pathway mis-regulation) besides contributing to adipocytes development *in vivo* [133]. We observed that C-MSCs might play a crucial role during AC-

correlated adipose substitution in human hearts. Indeed, we observed that C-MSCs isolated from human AC hearts are *in vitro* more prone than C-MSCs obtained from control hearts not only to accumulate fat (lipogenesis), but to specifically differentiate into adipocytes. These data are very important to define AC pathogenesis and their role should be more investigated to prevent the adipogenic substitution in AC patients' hearts. Besides C-MSCs role in AC we decided to evaluate miR-320a role during adipogenesis in C-MSCs. In basal conditions (T.MES), unexpectedly, AC C-MSCs showed a trend of lower miR-320a expression compared to NON-AC (Figure 26, panel A), as seen in plasma samples. Despite the strong consistency of results in plasma and cell model, we were expecting miR-320a expression of AC C-MSCs in basal medium higher than NON-AC, because of the predisposition of AC cells to adipogenesis. To explain these data we could speculate that a sort of protective mechanism is carried out by AC cells to control their genetic predisposition to fat accumulation by keeping miR-320a at low levels. This will be the subject of further in-depth-analysis. Nevertheless, during adipogenesis, miR-320a levels increased both in AC and NON-AC in C-MSCs (Figure 26, panel B), confirming literature data _ENREF_134. In this condition the difference between AC and NON-AC miRNA expression levelled (Figure 26, panel C), since miR-320a expression increased more in AC cells, as expected. This result is in agreement with the mis-regulation of the Wnt/β-catenin pathway in AC cells and with the interference of miRNAs in β-catenin expression. It will be very interesting to evaluate miR-320a expression in supernatants-derived RNA in order to elucidate putative release mechanisms that can recapitulate what we observed in plasma AC samples.

Despite our present results, our understanding of how miRNAs function in AC developmental and disease pathways is really far to be elucidated and numerous conceptual and experimental questions still remain unsolved. To date, only a handful of the hundreds of miRNAs expressed in cardiovascular system have been functionally analyzed. The ability of these miRNAs to fine-tune gene expression programs portends their importance in many facets of cardiac biology. It's a virtual certainty that many unexplored roles of miRNAs in control of normal and abnormal cardiac function are awaiting discovery. Our present findings are clearly an advances in understanding the role of miRNAs in pathological AC. In summary, to date studies have identified MiR-320a as a

candidate miRNAs which can accelerate adipocyte differentiation. These miRNAs may provide promising candidates to design specific drugs able to counteract the heart muscle to adipose tissue differentiation. However, it remains important to examine whether miRNAs and in particular MiR-320a which regulates adipocyte differentiation *in-vitro* are dysregulated in human AC *in-vivo*.

CONCLUSIONS

This is the first study identifying miR-320a as a possible new biomarker for the diagnosis of AC. In our cohort of patients the level of expression of miR-320a was constantly lower in patients with a diagnosis of AC than in controls and patients with ventricular arrhythmias with a different pathogenesis (IVT and IC). In particular, the expression of miR-320a has a fairly good accuracy in discriminating AC vs. IVT patients.

Unfortunately we did not find in the present research a clear statistical correlation between the level of expression of miR-320a and the severity of AC, but we believe the low number of examinated patients could be a bias for these results. Moreover we can speculate that miR-320a could be just a trigger or a co-factor of a more complex series of events leading to the development of the disease.

We showed how miR-320a is regulated during the adipogenic differentiation of C-CMSs which have been considered as a cardiac cellular model of AC, and this new findings for sure will pave the way to future mechanistic studies on the epigenetic control of AC structural and functional damages and in particular the fibro-fatty alteration.

The novelty of the present result and in particular our findings about the correlation with the expression of the miR-320a and the some of the most important feature of AC disease are of great importance and could justify future clinical trials aiming to unravel the unclear path of AC diagnosis.

This study is a clear example of a bench to bedside research approach, but the process of translating laboratory discovery into patient care is more complex and more varied than it might first appear.

This research work is also an example of how to approach translational research from various angles and coming up with innovative ways to overcome the many challenges of a very complex disease, which is Arrhythmogenic Cardiomyopathy. The close network collaboration between expert electrophysiologist, the molecular biology lab of the Monzino Cardiologic Center in Milan with the researchers of the Cardiovascular Pathology of Padova University, who starting from a clinical need, are attempting to

sinergically find a solution potentially useful for the clinical management of these so severe disease.

BIBLIOGRAPHY

1. Thiene G, Nava A, Corrado D, Rossi L, Pennelli N. Right ventricular cardiomyopathy and sudden death in young people. *N Engl J Med*. 1988;318:129-133

2. Marcus FI, Fontaine GH, Guiraudon G, Frank R, Laurenceau JL, Malergue C, Grosgogeat Y. Right ventricular dysplasia: A report of 24 adult cases. *Circulation*. 1982;65:384-398

3. Fontaine G, Guiraudon G, Frank R, Tereau Y, Fillette F, Marcus FI, Chomette G, Grosgogeat Y. [arrhythmogenic right ventricular dysplasia and uhl's disease]. *Archives des maladies du coeur et des vaisseaux*. 1982;75:361-371

4. Richardson P, McKenna W, Bristow M, Maisch B, Mautner B, O'Connell J, Olsen E, Thiene G, Goodwin J, Gyarfas I, Martin I, Nordet P. Report of the 1995 world health organization/international society and federation of cardiology task force on the definition and classification of cardiomyopathies. *Circulation*. 1996;93:841-842

5. Norman M, Simpson M, Mogensen J, Shaw A, Hughes S, Syrris P, Sen-Chowdhry S, Rowland E, Crosby A, McKenna WJ. Novel mutation in desmoplakin causes arrhythmogenic left ventricular cardiomyopathy. *Circulation*. 2005;112:636-642

6. Gear K, Marcus F. Arrhythmogenic right ventricular dysplasia/cardiomyopathy. *Circulation*. 2003;107:e31-33

7. Marcus FI, McKenna WJ, Sherrill D, Basso C, Bauce B, Bluemke DA, Calkins H, Corrado D, Cox MG, Daubert JP, Fontaine G, Gear K, Hauer R, Nava A, Picard MH, Protonotarios N, Saffitz JE, Sanborn DM, Steinberg JS, Tandri H, Thiene G, Towbin JA, Tsatsopoulou A, Wichter T, Zareba W. Diagnosis of arrhythmogenic right ventricular cardiomyopathy/dysplasia: Proposed modification of the task force criteria. *European heart journal*. 2010;31:806-814

8. Coumbe A, Perez-Martinez AL, Fegan AW, Hill IR. Arrhythmogenic right ventricular dysplasia (arvd): An overlooked and underdiagnosed condition? *Medicine, science, and the law*. 1997;37:262-265

9. Thiene G, Basso C, Danieli G, Rampazzo A, Corrado D, Nava A. Arrhythmogenic right ventricular cardiomyopathy a still underrecognized clinic entity. *Trends in cardiovascular medicine*. 1997;7:84-90

10. Marcus N, Thiene. *Arrhythmogenic right ventricular cardiomyopathy - dysplasia - recent advances*. 2007.

11. Sen-Chowdhry S, Syrris P, Prasad SK, Hughes SE, Merrifield R, Ward D, Pennell DJ, McKenna WJ. Left-dominant arrhythmogenic cardiomyopathy: An under-recognized clinical entity. *Journal of the American College of Cardiology*. 2008;52:2175-2187

12. Basso C, Thiene G, Corrado D, Angelini A, Nava A, Valente M. Arrhythmogenic right ventricular cardiomyopathy. Dysplasia, dystrophy, or myocarditis? *Circulation*. 1996;94:983-991

13. Basso C, Bauce B, Corrado D, Thiene G. Pathophysiology of arrhythmogenic cardiomyopathy. *Nature reviews. Cardiology*. 2012;9:223-233

14. Gemayel C, Pelliccia A, Thompson PD. Arrhythmogenic right ventricular cardiomyopathy. *J Am Coll Cardiol*. 2001;38:1773-1781

15. Peters S, Trummel M, Meyners W. Prevalence of right ventricular dysplasia-cardiomyopathy in a non-referral hospital. *Int J Cardiol*. 2004;97:499-501

16. Thiene G, Corrado D, Basso C. Arrhythmogenic right ventricular cardiomyopathy/dysplasia. *Orphanet J Rare Dis*. 2007;2:45

17. Migliore F, Zorzi A, Michieli P, Perazzolo Marra M, Siciliano M, Rigato I, Bauce B, Basso C, Toazza D, Schiavon M, Iliceto S, Thiene G, Corrado D. Prevalence of cardiomyopathy in italian asymptomatic children with electrocardiographic t-wave inversion at preparticipation screening. *Circulation*. 2012;125:529-538

18. Corrado D, Thiene G. Arrhythmogenic right ventricular cardiomyopathy/dysplasia: Clinical impact of molecular genetic studies. *Circulation*. 2006;113:1634-1637

19. Nava A, Thiene G, Canciani B, Scognamiglio R, Daliento L, Buja G, Martini B, Stritoni P, Fasoli G. Familial occurrence of right ventricular dysplasia: A study involving nine families. *Journal of the American College of Cardiology*. 1988;12:1222-1228

20. Protonotarios N, Tsatsopoulou A, Fontaine G. Naxos disease: Keratoderma, scalp modifications, and cardiomyopathy. *J Am Acad Dermatol*. 2001;44:309-311

21. Norgett EE, Hatsell SJ, Carvajal-Huerta L, Cabezas JC, Common J, Purkis PE, Whittock N, Leigh IM, Stevens HP, Kelsell DP. Recessive mutation in desmoplakin disrupts desmoplakin-intermediate filament interactions and causes dilated cardiomyopathy, woolly hair and keratoderma. *Human molecular genetics*. 2000;9:2761-2766

22. McKoy G, Protonotarios N, Crosby A, Tsatsopoulou A, Anastasakis A, Coonar A, Norman M, Baboonian C, Jeffery S, McKenna WJ. Identification of a deletion in plakoglobin in arrhythmogenic right ventricular cardiomyopathy with palmoplantar keratoderma and woolly hair (naxos disease). *Lancet*. 2000;355:2119-2124

23. Gerull B, Heuser A, Wichter T, Paul M, Basson CT, McDermott DA, Lerman BB, Markowitz SM, Ellinor PT, MacRae CA, Peters S, Grossmann KS, Drenckhahn J, Michely B, Sasse-Klaassen S, Birchmeier W, Dietz R, Breithardt G, Schulze-Bahr E, Thierfelder L. Mutations in the desmosomal protein plakophilin-2 are common in arrhythmogenic right ventricular cardiomyopathy. *Nature genetics*. 2004;36:1162-1164

24. Awad MM, Dalal D, Tichnell C, James C, Tucker A, Abraham T, Spevak PJ, Calkins H, Judge DP. Recessive arrhythmogenic right ventricular dysplasia due to novel cryptic splice mutation in pkp2. *Human mutation*. 2006;27:1157

25. Pilichou K, Nava A, Basso C, Beffagna G, Bauce B, Lorenzon A, Frigo G, Vettori A, Valente M, Towbin J, Thiene G, Danieli GA, Rampazzo A. Mutations in desmoglein-2 gene are associated with arrhythmogenic right ventricular cardiomyopathy. *Circulation*. 2006;113:1171-1179

26. Syrris P, Ward D, Evans A, Asimaki A, Gandjbakhch E, Sen-Chowdhry S, McKenna WJ. Arrhythmogenic right ventricular dysplasia/cardiomyopathy associated with mutations in the desmosomal gene desmocollin-2. *Am J Hum Genet*. 2006;79:978-984

27. Keller DI, Stepowski D, Balmer C, Simon F, Guenthard J, Bauer F, Itin P, David N, Drouin-Garraud V, Fressart V. De novo heterozygous desmoplakin mutations leading to naxos-carvajal disease. *Swiss medical weekly*. 2012;142:w13670

28. Basso C, Corrado D, Marcus FI, Nava A, Thiene G. Arrhythmogenic right ventricular cardiomyopathy. *Lancet*. 2009;373:1289-1300

29. Garcia-Gras E, Lombardi R, Giocondo MJ, Willerson JT, Schneider MD, Khoury DS, Marian AJ. Suppression of canonical wnt/beta-catenin signaling by nuclear plakoglobin recapitulates phenotype of arrhythmogenic right ventricular cardiomyopathy. *The Journal of clinical investigation*. 2006;116:2012-2021

30. MacRae CA, Birchmeier W, Thierfelder L. Arrhythmogenic right ventricular cardiomyopathy: Moving toward mechanism. *The Journal of clinical investigation*. 2006;116:1825-1828

31. Beffagna G, Occhi G, Nava A, Vitiello L, Ditadi A, Basso C, Bauce B, Carraro G, Thiene G, Towbin JA, Danieli GA, Rampazzo A. Regulatory mutations in transforming growth factor-beta3 gene cause arrhythmogenic right ventricular cardiomyopathy type 1. *Cardiovasc Res*. 2005;65:366-373

32. Tiso N, Stephan DA, Nava A, Bagattin A, Devaney JM, Stanchi F, Larderet G, Brahmbhatt B, Brown K, Bauce B, Muriago M, Basso C, Thiene G, Danieli GA, Rampazzo A. Identification of mutations in the cardiac ryanodine receptor gene in families affected with arrhythmogenic right ventricular cardiomyopathy type 2 (arvd2). *Hum Mol Genet*. 2001;10:189-194

33. Priori SG, Napolitano C, Tiso N, Memmi M, Vignati G, Bloise R, Sorrentino V, Danieli GA. Mutations in the cardiac ryanodine receptor gene (hryr2) underlie catecholaminergic polymorphic ventricular tachycardia. *Circulation*. 2001;103:196-200

34. Christensen AH, Andersen CB, Tybjaerg-Hansen A, Haunso S, Svendsen JH. Mutation analysis and evaluation of the cardiac localization of tmem43 in arrhythmogenic right ventricular cardiomyopathy. *Clin Genet*. 2011;80:256-264

35. Klauke B, Kossmann S, Gaertner A, Brand K, Stork I, Brodehl A, Dieding M, Walhorn V, Anselmetti D, Gerdes D, Bohms B, Schulz U, Zu Knyphausen E, Vorgerd M, Gummert J, Milting H. De novo desmin-mutation n116s is associated with arrhythmogenic right ventricular cardiomyopathy. *Hum Mol Genet*. 2010;19:4595-4607

36. Lapouge K, Fontao L, Champliaud MF, Jaunin F, Frias MA, Favre B, Paulin D, Green KJ, Borradori L. New insights into the molecular basis of desmoplakin- and desmin-related cardiomyopathies. *J Cell Sci*. 2006;119:4974-4985

37. Taylor M, Graw S, Sinagra G, Barnes C, Slavov D, Brun F, Pinamonti B, Salcedo EE, Sauer W, Pyxaras S, Anderson B, Simon B, Bogomolovas J, Labeit S, Granzier H, Mestroni L. Genetic variation in titin in arrhythmogenic right ventricular cardiomyopathy-overlap syndromes. *Circulation*. 2011;124:876-885

38. LeWinter MM, Granzier HL. Cardiac titin and heart disease. *J Cardiovasc Pharmacol*. 2014;63:207-212

39. Anderson BR, Bogomolovas J, Labeit S, Granzier H. Single molecule force spectroscopy on titin implicates immunoglobulin domain stability as a cardiac disease mechanism. *The Journal of biological chemistry*. 2013;288:5303-5315

40. van der Zwaag PA, van Rijsingen IA, Asimaki A, Jongbloed JD, van Veldhuisen DJ, Wiesfeld AC, Cox MG, van Lochem LT, de Boer RA, Hofstra RM, Christiaans I, van Spaendonck-Zwarts KY, Lekanne dit Deprez RH, Judge DP, Calkins H, Suurmeijer AJ, Hauer RN, Saffitz JE, Wilde AA, van den Berg MP, van Tintelen JP. Phospholamban r14del mutation in patients diagnosed with dilated cardiomyopathy or arrhythmogenic right ventricular cardiomyopathy: Evidence supporting the concept of arrhythmogenic cardiomyopathy. *Eur J Heart Fail*. 2012;14:1199-1207

41. Valtuille L, Paterson I, Kim DH, Mullen J, Sergi C, Oudit GY. A case of lamin a/c mutation cardiomyopathy with overlap features of arvc: A critical role of genetic testing. *Int J Cardiol*. 2013;168:4325-4327

42. Lilien J, Balsamo J. The regulation of cadherin-mediated adhesion by tyrosine phosphorylation/dephosphorylation of beta-catenin. *Curr Opin Cell Biol*. 2005;17:459-465

43. Venkiteswaran K, Xiao K, Summers S, Calkins CC, Vincent PA, Pumiglia K, Kowalczyk AP. Regulation of endothelial barrier function and growth by ve-cadherin, plakoglobin, and beta-catenin. *Am J Physiol Cell Physiol*. 2002;283:C811-821

44. Reya T, Clevers H. Wnt signalling in stem cells and cancer. *Nature*. 2005;434:843-850

45. Doucas H, Garcea G, Neal CP, Manson MM, Berry DP. Changes in the wnt signalling pathway in gastrointestinal cancers and their prognostic significance. *Eur J Cancer*. 2005;41:365-379

46. Gregorieff A, Clevers H. Wnt signaling in the intestinal epithelium: From endoderm to cancer. *Genes Dev*. 2005;19:877-890

47. Wang J, Wynshaw-Boris A. The canonical wnt pathway in early mammalian embryogenesis and stem cell maintenance/differentiation. *Curr Opin Genet Dev*. 2004;14:533-539

48. Eisenberg LM, Eisenberg CA. Wnt signal transduction and the formation of the myocardium. *Dev Biol*. 2006;293:305-315

49. Bennett CN, Ross SE, Longo KA, Bajnok L, Hemati N, Johnson KW, Harrison SD, MacDougald OA. Regulation of wnt signaling during adipogenesis. *J Biol Chem*. 2002;277:30998-31004

50. Bhanot P, Brink M, Samos CH, Hsieh JC, Wang Y, Macke JP, Andrew D, Nathans J, Nusse R. A new member of the frizzled family from drosophila functions as a wingless receptor. *Nature*. 1996;382:225-230

51. Bejsovec A. Wnt signaling: An embarrassment of receptors. *Curr Biol*. 2000;10:R919-922

52. Papkoff J, Aikawa M. Wnt-1 and hgf regulate gsk3 beta activity and beta-catenin signaling in mammary epithelial cells. *Biochem Biophys Res Commun*. 1998;247:851-858

53. Aberle H, Bauer A, Stappert J, Kispert A, Kemler R. Beta-catenin is a target for the ubiquitin-proteasome pathway. *The EMBO journal*. 1997;16:3797-3804

54. Cristancho AG, Lazar MA. Forming functional fat: A growing understanding of adipocyte differentiation. *Nat Rev Mol Cell Biol*. 2011;12:722-734

55. Deb A. Cell-cell interaction in the heart via wnt/beta-catenin pathway after cardiac injury. *Cardiovasc Res*. 2014;102:214-223

56. Lombardi R, da Graca Cabreira-Hansen M, Bell A, Fromm RR, Willerson JT, Marian AJ. Nuclear plakoglobin is essential for differentiation of cardiac progenitor cells to adipocytes in arrhythmogenic right ventricular cardiomyopathy. *Circulation research*. 2011;109:1342-1353

57. Marcus FI, Abidov A. Arrhythmogenic right ventricular cardiomyopathy 2012: Diagnostic challenges and treatment. *J Cardiovasc Electrophysiol*. 2012;23:1149-1153

58. James CA, Calkins H. Update on arrhythmogenic right ventricular dysplasia/cardiomyopathy (arvd/c). *Current treatment options in cardiovascular medicine*. 2013;15:476-487

59. Avella A, d'Amati G, Tondo C. Diagnosis of arrhythmogenic right ventricular cardiomyopathy: The role of endomyocardial biopsy guided by electroanatomic voltage map. *Europace*. 2009;11:970; author reply 970-971

60. Asimaki A, Tandri H, Huang H, Halushka MK, Gautam S, Basso C, Thiene G, Tsatsopoulou A, Protonotarios N, McKenna WJ, Calkins H, Saffitz JE. A new

diagnostic test for arrhythmogenic right ventricular cardiomyopathy. *N Engl J Med*. 2009;360:1075-1084

61. Kwon YS, Park TI, Cho Y, Bae MH, Kim S. Clinical usefulness of immunohistochemistry for plakoglobin, n-cadherin, and connexin-43 in the diagnosis of arrhythmogenic right ventricular cardiomyopathy. *Int J Clin Exp Pathol*. 2013;6:2928-2935

62. Asimaki A, Tandri H, Duffy ER, Winterfield JR, Mackey-Bojack S, Picken MM, Cooper LT, Wilber DJ, Marcus FI, Basso C, Thiene G, Tsatsopoulou A, Protonotarios N, Stevenson WG, McKenna WJ, Gautam S, Remick DG, Calkins H, Saffitz JE. Altered desmosomal proteins in granulomatous myocarditis and potential pathogenic links to arrhythmogenic right ventricular cardiomyopathy. *Circ Arrhythm Electrophysiol*. 2011;4:743-752

63. Hong TT, Cogswell R, James CA, Kang G, Pullinger CR, Malloy MJ, Kane JP, Wojciak J, Calkins H, Scheinman MM, Tseng ZH, Ganz P, De Marco T, Judge DP, Shaw RM. Plasma bin1 correlates with heart failure and predicts arrhythmia in patients with arrhythmogenic right ventricular cardiomyopathy. *Heart Rhythm*. 2012;9:961-967

64. Avella A, d'Amati G, Pappalardo A, Re F, Silenzi PF, Laurenzi F, P DEG, Pelargonio G, Dello Russo A, Baratta P, Messina G, Zecchi P, Zachara E, Tondo C. Diagnostic value of endomyocardial biopsy guided by electroanatomic voltage mapping in arrhythmogenic right ventricular cardiomyopathy/dysplasia. *J Cardiovasc Electrophysiol*. 2008;19:1127-1134

65. Casella M, Pizzamiglio F, Dello Russo A, Carbucicchio C, Al-Mohani G, Russo E, Notarstefano P, Pieroni M, D'Amati G, Sommariva E, Giovannardi M, Carnevali A, Riva S, Fassini G, Tundo F, Santangeli P, Di Biase L, Bolognese L, Natale A, Tondo C. Feasibility of combined unipolar and bipolar voltage maps to improve sensitivity of endomyocardial biopsy. *Circ Arrhythm Electrophysiol*. 2015

66. Corrado D, Basso C, Leoni L, Tokajuk B, Bauce B, Frigo G, Tarantini G, Napodano M, Turrini P, Ramondo A, Daliento L, Nava A, Buja G, Iliceto S, Thiene G. Three-dimensional electroanatomic voltage mapping increases accuracy of diagnosing arrhythmogenic right ventricular cardiomyopathy/dysplasia. *Circulation*. 2005;111:3042-3050

67. Lacroix D, Lions C, Klug D, Prat A. Arrhythmogenic right ventricular dysplasia: Catheter ablation, mri, and heart transplantation. *J Cardiovasc Electrophysiol*. 2005;16:235-236

68. Kottkamp H, Hindricks G. Catheter ablation of ventricular tachycardia in arvc: Is curative treatment at the horizon? *J Cardiovasc Electrophysiol*. 2006;17:477-479

69. Karchmer AW, Longworth DL. Infections of intracardiac devices. *Infect Dis Clin North Am*. 2002;16:477-505, xii

70. Pavia S, Wilkoff B. The management of surgical complications of pacemaker and implantable cardioverter-defibrillators. *Curr Opin Cardiol*. 2001;16:66-71

71. Lichtman JH, Naert L, Allen NB, Watanabe E, Jones SB, Barry LC, Bravata DM, Goldstein LB. Use of antithrombotic medications among elderly ischemic stroke patients. *Circ Cardiovasc Qual Outcomes*. 2011;4:30-38

72. Corrado D, Leoni L, Link MS, Della Bella P, Gaita F, Curnis A, Salerno JU, Igidbashian D, Raviele A, Disertori M, Zanotto G, Verlato R, Vergara G, Delise P, Turrini P, Basso C, Naccarella F, Maddalena F, Estes NA, 3rd, Buja G, Thiene G. Implantable cardioverter-defibrillator therapy for prevention of sudden death in patients with arrhythmogenic right ventricular cardiomyopathy/dysplasia. *Circulation*. 2003;108:3084-3091

73. Bhonsale A, James CA, Tichnell C, Murray B, Gagarin D, Philips B, Dalal D, Tedford R, Russell SD, Abraham T, Tandri H, Judge DP, Calkins H. Incidence and predictors of implantable cardioverter-defibrillator therapy in patients with arrhythmogenic right ventricular dysplasia/cardiomyopathy undergoing implantable cardioverter-defibrillator implantation for primary prevention. *Journal of the American College of Cardiology*. 2011;58:1485-1496

74. Link MS, Laidlaw D, Polonsky B, Zareba W, McNitt S, Gear K, Marcus F, Estes NA, 3rd. Ventricular arrhythmias in the north american multidisciplinary study of arvc: Predictors, characteristics, and treatment. *J Am Coll Cardiol*. 2014;64:119-125

75. Saguner AM, Vecchiati A, Baldinger SH, Rueger S, Medeiros-Domingo A, Mueller-Burri AS, Haegeli LM, Biaggi P, Manka R, Luscher TF, Fontaine G, Delacretaz E, Jenni R, Held L, Brunckhorst C, Duru F, Tanner FC. Different prognostic value of functional right ventricular parameters in arrhythmogenic right ventricular cardiomyopathy/dysplasia. *Circ Cardiovasc Imaging*. 2014;7:230-239

76. Santangeli P, Dello Russo A, Pieroni M, Casella M, Di Biase L, Burkhardt JD, Sanchez J, Lakkireddy D, Carbucicchio C, Zucchetti M, Pelargonio G, Themistoclakis S, Camporeale A, Rossillo A, Beheiry S, Hongo R, Bellocci F, Tondo C, Natale A. Fragmented and delayed electrograms within fibrofatty scar predict arrhythmic events in arrhythmogenic right ventricular cardiomyopathy:

Results from a prospective risk stratification study. *Heart Rhythm*. 2012;9:1200-1206

77. Zipes DP, Camm AJ, Borggrefe M, Buxton AE, Chaitman B, Fromer M, Gregoratos G, Klein G, Moss AJ, Myerburg RJ, Priori SG, Quinones MA, Roden DM, Silka MJ, Tracy C, Smith SC, Jr., Jacobs AK, Adams CD, Antman EM, Anderson JL, Hunt SA, Halperin JL, Nishimura R, Ornato JP, Page RL, Riegel B, Blanc JJ, Budaj A, Dean V, Deckers JW, Despres C, Dickstein K, Lekakis J, McGregor K, Metra M, Morais J, Osterspey A, Tamargo JL, Zamorano JL. Acc/aha/esc 2006 guidelines for management of patients with ventricular arrhythmias and the prevention of sudden cardiac death: A report of the american college of cardiology/american heart association task force and the european society of cardiology committee for practice guidelines (writing committee to develop guidelines for management of patients with ventricular arrhythmias and the prevention of sudden cardiac death): Developed in collaboration with the european heart rhythm association and the heart rhythm society. *Circulation*. 2006;114:e385-484

78. Lee RC, Ambros V. An extensive class of small rnas in caenorhabditis elegans. *Science*. 2001;294:862-864

79. van Rooij E. The art of microrna research. *Circulation research*. 2011;108:219-234

80. Reinhart BJ, Weinstein EG, Rhoades MW, Bartel B, Bartel DP. Micrornas in plants. *Genes Dev*. 2002;16:1616-1626

81. Chen CZ, Li L, Lodish HF, Bartel DP. Micrornas modulate hematopoietic lineage differentiation. *Science*. 2004;303:83-86

82. Xu P, Vernooy SY, Guo M, Hay BA. The drosophila microrna mir-14 suppresses cell death and is required for normal fat metabolism. *Curr Biol*. 2003;13:790-795

83. Bueno MJ, Perez de Castro I, Malumbres M. Control of cell proliferation pathways by micrornas. *Cell Cycle*. 2008;7:3143-3148

84. Fabbri M, Paone A, Calore F, Galli R, Croce CM. A new role for micrornas, as ligands of toll-like receptors. *RNA Biol*. 2013;10:169-174

85. Blanchette M, Labourier E, Green RE, Brenner SE, Rio DC. Genome-wide analysis reveals an unexpected function for the drosophila splicing factor u2af50 in the nuclear export of intronless mrnas. *Mol Cell*. 2004;14:775-786

86. Hayashita Y, Osada H, Tatematsu Y, Yamada H, Yanagisawa K, Tomida S, Yatabe Y, Kawahara K, Sekido Y, Takahashi T. A polycistronic microrna cluster, mir-17-92, is overexpressed in human lung cancers and enhances cell proliferation. *Cancer Res*. 2005;65:9628-9632

87. D'Alessandra Y, Devanna P, Limana F, Straino S, Di Carlo A, Brambilla PG, Rubino M, Carena MC, Spazzafumo L, De Simone M, Micheli B, Biglioli P, Achilli F, Martelli F, Maggiolini S, Marenzi G, Pompilio G, Capogrossi MC. Circulating microrna are new and sensitive biomarkers of myocardial infarction. *Eur Heart J*. 2010;31:2765-2773

88. Khraiwesh B, Arif MA, Seumel GI, Ossowski S, Weigel D, Reski R, Frank W. Transcriptional control of gene expression by microrna. *Cell*. 2010;140:111-122

89. Gonzalez S, Pisano DG, Serrano M. Mechanistic principles of chromatin remodeling guided by sirna and mirna. *Cell Cycle*. 2008;7:2601-2608

90. Kim DH, Saetrom P, Snove O, Jr., Rossi JJ. Microrna-directed transcriptional gene silencing in mammalian cells. *Proc Natl Acad Sci U S A*. 2008;105:16230-16235

91. Orom UA, Nielsen FC, Lund AH. Microrna-10a binds the 5'utr of ribosomal protein mrnas and enhances their translation. *Mol Cell*. 2008;30:460-471

92. Winter J, Jung S, Keller S, Gregory RI, Diederichs S. Many roads to maturity: Microrna biogenesis pathways and their regulation. *Nat Cell Biol*. 2009;11:228-234

93. Lee Y, Kim M, Han J, Yeom KH, Lee S, Baek SH, Kim VN. Microrna genes are transcribed by rna polymerase ii. *EMBO J*. 2004;23:4051-4060

94. Borchert GM, Lanier W, Davidson BL. Rna polymerase iii transcribes human micrornas. *Nat Struct Mol Biol*. 2006;13:1097-1101

95. Cai X, Hagedorn CH, Cullen BR. Human micrornas are processed from capped, polyadenylated transcripts that can also function as mrnas. *RNA*. 2004;10:1957-1966

96. Saini HK, Griffiths-Jones S, Enright AJ. Genomic analysis of human microrna transcripts. *Proc Natl Acad Sci U S A*. 2007;104:17719-17724

97. Han J, Lee Y, Yeom KH, Nam JW, Heo I, Rhee JK, Sohn SY, Cho Y, Zhang BT, Kim VN. Molecular basis for the recognition of primary micrornas by the drosha-dgcr8 complex. *Cell*. 2006;125:887-901

98. Lee Y, Ahn C, Han J, Choi H, Kim J, Yim J, Lee J, Provost P, Radmark O, Kim S, Kim VN. The nuclear rnase iii drosha initiates microrna processing. *Nature*. 2003;425:415-419

99. Yi R, Qin Y, Macara IG, Cullen BR. Exportin-5 mediates the nuclear export of pre-microrna and short hairpin rnas. *Genes Dev*. 2003;17:3011-3016

100. Zeng Y, Cullen BR. Structural requirements for pre-microrna binding and nuclear export by exportin 5. *Nucleic Acids Res*. 2004;32:4776-4785

101. Matranga C, Tomari Y, Shin C, Bartel DP, Zamore PD. Passenger-strand cleavage facilitates assembly of sirna into ago2-containing rnai enzyme complexes. *Cell*. 2005;123:607-620

102. Kozomara A, Griffiths-Jones S. Mirbase: Integrating microrna annotation and deep-sequencing data. *Nucleic Acids Res*. 2011;39:D152-157

103. He L, Hannon GJ. Micrornas: Small rnas with a big role in gene regulation. *Nat Rev Genet*. 2004;5:522-531

104. Lytle JR, Yario TA, Steitz JA. Target mrnas are repressed as efficiently by microrna-binding sites in the 5' utr as in the 3' utr. *Proc Natl Acad Sci U S A*. 2007;104:9667-9672

105. Duursma AM, Kedde M, Schrier M, le Sage C, Agami R. Mir-148 targets human dnmt3b protein coding region. *RNA*. 2008;14:872-877

106. Hsu SD, Chu CH, Tsou AP, Chen SJ, Chen HC, Hsu PW, Wong YH, Chen YH, Chen GH, Huang HD. Mirnamap 2.0: Genomic maps of micrornas in metazoan genomes. *Nucleic Acids Res*. 2008;36:D165-169

107. Creemers EE, Tijsen AJ, Pinto YM. Circulating micrornas: Novel biomarkers and extracellular communicators in cardiovascular disease? *Circulation research*. 2012;110:483-495

108. Gallo A, Tandon M, Alevizos I, Illei GG. The majority of micrornas detectable in serum and saliva is concentrated in exosomes. *PLoS One*. 2012;7:e30679

109. Diehl P, Fricke A, Sander L, Stamm J, Bassler N, Htun N, Ziemann M, Helbing T, El-Osta A, Jowett JB, Peter K. Microparticles: Major transport vehicles for distinct micrornas in circulation. *Cardiovasc Res*. 2012;93:633-644

110. Vickers KC, Palmisano BT, Shoucri BM, Shamburek RD, Remaley AT. Micrornas are transported in plasma and delivered to recipient cells by high-density lipoproteins. *Nat Cell Biol*. 2011;13:423-433

111. Arroyo JD, Chevillet JR, Kroh EM, Ruf IK, Pritchard CC, Gibson DF, Mitchell PS, Bennett CF, Pogosova-Agadjanyan EL, Stirewalt DL, Tait JF, Tewari M. Argonaute2 complexes carry a population of circulating micrornas independent of vesicles in human plasma. *Proceedings of the National Academy of Sciences of the United States of America*. 2011;108:5003-5008

112. Cortez MA, Bueso-Ramos C, Ferdin J, Lopez-Berestein G, Sood AK, Calin GA. Micrornas in body fluids--the mix of hormones and biomarkers. *Nat Rev Clin Oncol*. 2011;8:467-477

113. Fichtlscherer S, Zeiher AM, Dimmeler S. Circulating micrornas: Biomarkers or mediators of cardiovascular diseases? *Arterioscler Thromb Vasc Biol*. 2011;31:2383-2390

114. Hornby RJ, Starkey Lewis P, Dear J, Goldring C, Park BK. Micrornas as potential circulating biomarkers of drug-induced liver injury: Key current and future issues for translation to humans. *Expert Rev Clin Pharmacol*. 2014;7:349-362

115. Wang K, Zhang S, Marzolf B, Troisch P, Brightman A, Hu Z, Hood LE, Galas DJ. Circulating micrornas, potential biomarkers for drug-induced liver injury. *Proc Natl Acad Sci U S A*. 2009;106:4402-4407

116. Zampetaki A, Kiechl S, Drozdov I, Willeit P, Mayr U, Prokopi M, Mayr A, Weger S, Oberhollenzer F, Bonora E, Shah A, Willeit J, Mayr M. Plasma microrna profiling reveals loss of endothelial mir-126 and other micrornas in type 2 diabetes. *Circulation research*. 2010;107:810-817

117. Cermelli S, Ruggieri A, Marrero JA, Ioannou GN, Beretta L. Circulating micrornas in patients with chronic hepatitis c and non-alcoholic fatty liver disease. *PLoS One*. 2011;6:e23937

118. Xu J, Wu C, Che X, Wang L, Yu D, Zhang T, Huang L, Li H, Tan W, Wang C, Lin D. Circulating micrornas, mir-21, mir-122, and mir-223, in patients with hepatocellular carcinoma or chronic hepatitis. *Mol Carcinog*. 2011;50:136-142

119. Wang JF, Yu ML, Yu G, Bian JJ, Deng XM, Wan XJ, Zhu KM. Serum mir-146a and mir-223 as potential new biomarkers for sepsis. *Biochem Biophys Res Commun*. 2010;394:184-188

120. Iguchi H, Kosaka N, Ochiya T. Secretory micrornas as a versatile communication tool. *Commun Integr Biol*. 2010;3:478-481

121. Tijsen AJ, Pinto YM, Creemers EE. Circulating micrornas as diagnostic biomarkers for cardiovascular diseases. *Am J Physiol Heart Circ Physiol*. 2012;303:H1085-1095

122. Lu Y, Hou S, Huang D, Luo X, Zhang J, Chen J, Xu W. Expression profile analysis of circulating micrornas and their effects on ion channels in chinese atrial fibrillation patients. *Int J Clin Exp Med*. 2015;8:845-853

123. McManus DD, Lin H, Tanriverdi K, Quercio M, Yin X, Larson MG, Ellinor PT, Levy D, Freedman JE, Benjamin EJ. Relations between circulating micrornas and atrial fibrillation: Data from the framingham offspring study. *Heart Rhythm*. 2014;11:663-669

124. Friedenstein AJ, Deriglasova UF, Kulagina NN, Panasuk AF, Rudakowa SF, Luria EA, Ruadkow IA. Precursors for fibroblasts in different populations of hematopoietic cells as detected by the in vitro colony assay method. *Exp Hematol*. 1974;2:83-92

125. Pittenger MF, Mackay AM, Beck SC, Jaiswal RK, Douglas R, Mosca JD, Moorman MA, Simonetti DW, Craig S, Marshak DR. Multilineage potential of adult human mesenchymal stem cells. *Science*. 1999;284:143-147

126. Im GI, Shin YW, Lee KB. Do adipose tissue-derived mesenchymal stem cells have the same osteogenic and chondrogenic potential as bone marrow-derived cells? *Osteoarthritis Cartilage*. 2005;13:845-853

127. Campagnoli C, Roberts IA, Kumar S, Bennett PR, Bellantuono I, Fisk NM. Identification of mesenchymal stem/progenitor cells in human first-trimester fetal blood, liver, and bone marrow. *Blood*. 2001;98:2396-2402

128. Kawashima N. Characterisation of dental pulp stem cells: A new horizon for tissue regeneration? *Arch Oral Biol*. 2012;57:1439-1458

129. Kaplan JM, Youd ME, Lodie TA. Immunomodulatory activity of mesenchymal stem cells. *Curr Stem Cell Res Ther*. 2011;6:297-316

130. Rossini A, Frati C, Lagrasta C, Graiani G, Scopece A, Cavalli S, Musso E, Baccarin M, Di Segni M, Fagnoni F, Germani A, Quaini E, Mayr M, Xu Q, Barbuti A, DiFrancesco D, Pompilio G, Quaini F, Gaetano C, Capogrossi MC. Human

cardiac and bone marrow stromal cells exhibit distinctive properties related to their origin. *Cardiovasc Res*. 2011;89:650-660

131. Jugdutt BI. Ventricular remodeling after infarction and the extracellular collagen matrix: When is enough enough? *Circulation*. 2003;108:1395-1403

132. Brown RD, Ambler SK, Mitchell MD, Long CS. The cardiac fibroblast: Therapeutic target in myocardial remodeling and failure. *Annu Rev Pharmacol Toxicol*. 2005;45:657-687

133. Sommariva EB, S.; Carbucicchio, C.; Gambini, E.; Meraviglia, V.; Dello Russo, A.; Farina, F.; Casella, M.; Cogliati, E.; Paolin, A.; Ouali Alami, N.; Preziuso, C.; d'Amati, G.; Chen, H.S.V.; Rossini, A.; Capogrossi, M.C.; Tondo, C.; Pompilio, G. Cardiac mesenchymal stromal cells are a source of adipocytes in arrhythmogenic cardiomyopathy *Eur Heart J*. 2015;under revision

134. Hsieh IS, Chang KC, Tsai YT, Ke JY, Lu PJ, Lee KH, Yeh SD, Hong TM, Chen YL. Microrna-320 suppresses the stem cell-like characteristics of prostate cancer cells by downregulating the wnt/beta-catenin signaling pathway. *Carcinogenesis*. 2013;34:530-538

135. Ross SE, Hemati N, Longo KA, Bennett CN, Lucas PC, Erickson RL, MacDougald OA. Inhibition of adipogenesis by wnt signaling. *Science*. 2000;289:950-953

136. Etheridge SL, Spencer GJ, Heath DJ, Genever PG. Expression profiling and functional analysis of wnt signaling mechanisms in mesenchymal stem cells. *Stem Cells*. 2004;22:849-860

137. Hamam D, Ali D, Vishnubalaji R, Hamam R, Al-Nbaheen M, Chen L, Kassem M, Aldahmash A, Alajez NM. Microrna-320/runx2 axis regulates adipocytic differentiation of human mesenchymal (skeletal) stem cells. *Cell Death Dis*. 2014;5:e1499

138. Beltrami AP, Cesselli D, Bergamin N, Marcon P, Rigo S, Puppato E, D'Aurizio F, Verardo R, Piazza S, Pignatelli A, Poz A, Baccarani U, Damiani D, Fanin R, Mariuzzi L, Finato N, Masolini P, Burelli S, Belluzzi O, Schneider C, Beltrami CA. Multipotent cells can be generated in vitro from several adult human organs (heart, liver, and bone marrow). *Blood*. 2007;110:3438-3446

139. Woeller CF, O'Loughlin CW, Pollock SJ, Thatcher TH, Feldon SE, Phipps RP. Thy1 (cd90) controls adipogenesis by regulating activity of the src family kinase, fyn. *FASEB J*. 2015;29:920-931

140. Rege TA, Hagood JS. Thy-1 as a regulator of cell-cell and cell-matrix interactions in axon regeneration, apoptosis, adhesion, migration, cancer, and fibrosis. *FASEB J*. 2006;20:1045-1054

141. Saberniak J, Hasselberg NE, Borgquist R, Platonov PG, Sarvari SI, Smith HJ, Ribe M, Holst AG, Edvardsen T, Haugaa KH. Vigorous physical activity impairs myocardial function in patients with arrhythmogenic right ventricular cardiomyopathy and in mutation positive family members. *Eur J Heart Fail*. 2014;16:1337-1344

142. Behr ER, Dalageorgou C, Christiansen M, Syrris P, Hughes S, Tome Esteban MT, Rowland E, Jeffery S, McKenna WJ. Sudden arrhythmic death syndrome: Familial evaluation identifies inheritable heart disease in the majority of families. *Eur Heart J*. 2008;29:1670-1680

143. Heidbuchel H, La Gerche A. The right heart in athletes. Evidence for exercise-induced arrhythmogenic right ventricular cardiomyopathy. *Herzschrittmacherther Elektrophysiol*. 2012;23:82-86

144. Sharma S, Papadakis M, Whyte G. Chronic ultra-endurance exercise: Implications in arrhythmogenic substrates in previously normal hearts. *Heart*. 2010;96:1255-1256

145. Ling HY, Ou HS, Feng SD, Zhang XY, Tuo QH, Chen LX, Zhu BY, Gao ZP, Tang CK, Yin WD, Zhang L, Liao DF. Changes in microrna (mir) profile and effects of mir-320 in insulin-resistant 3t3-l1 adipocytes. *Clin Exp Pharmacol Physiol*. 2009;36:e32-39